

# Thirteenth-century stained glass windows of the Sainte-Chapelle in Paris: an insight into medieval glazing work practices

Myrtille O.J.Y. Hunault, Fanny Bauchau, Karine Boulanger, Michel Hérold, Georges Calas, Quentin Lemasson, Laurent Pichon, Claire Pacheco, Claudine Loisel

▶ **To cite this version:**

Myrtille O.J.Y. Hunault, Fanny Bauchau, Karine Boulanger, Michel Hérold, Georges Calas, et al.. Thirteenth-century stained glass windows of the Sainte-Chapelle in Paris: an insight into medieval glazing work practices. Journal of Archaeological Science: Reports, 2021, 35, pp.102753. 10.1016/j.jasrep.2020.102753 . hal-03292392

**HAL Id: hal-03292392**

**https://hal.sorbonne-universite.fr/hal-03292392**

Submitted on 20 Jul 2021

**HAL** is a multi-disciplinary open access archive for the deposit and dissemination of scientific research documents, whether they are published or not. The documents may come from teaching and research institutions in France or abroad, or from public or private research centers.

L'archive ouverte pluridisciplinaire **HAL**, est destinée au dépôt et à la diffusion de documents scientifiques de niveau recherche, publiés ou non, émanant des établissements d'enseignement et de recherche français ou étrangers, des laboratoires publics ou privés.

# Thirteenth-century stained glass windows of the Sainte-Chapelle in Paris: an insight into medieval glazing work practices

Myrtille O.J.Y. Hunault,[a,b,d,1] Fanny Bauchau,[a,b,2] Karine Boulanger,[c] Michel Hérold,[c] Georges Calas,[d] Quentin Lemasson,[e,f] Laurent Pichon,[e,f] Claire Pacheco,[e,f] and Claudine Loisel[a,b]

[a,] Laboratoire de Recherche des Monuments Historiques, Ministère de la Culture, 77400 Champs-sur-Marne, France
[b,] Centre de Recherche sur la Conservation (CRC), Muséum National d'Histoire Naturelle, CNRS, Ministère de la Culture, Paris, France
[c,] Centre André Chastel, Sorbonne Université, 2 rue Vivienne, 75002 Paris, France
[d] Institut de Minéralogie et de Physique des Matériaux et de Cosmochimie, Sorbonne Université, Place Jussieu, 75005 Paris, France
[e,] Centre de recherche et de restauration des musées de France, Palais du Louvre, 14 quai François Mitterrand, 75001 Paris, France
f, New AGLAE FR 3506 – Chimie-Paristech/Ministère de la Culture et de la Communication, Palais du Louvre, 14 Quai F. Mitterrand, Paris 75001, France

[1]Present address: Synchrotron SOLEIL, L'Orme des Merisiers, Saint-Aubin, 91192 Gif-sur-Yvette, France ;
[2]Present address: CICRP 21, rue Guibal, 13003 MARSEILLE, FRANCE

## Abstract

The restoration of the four northern windows of the 13th century Sainte-Chapelle in Paris from 2011 to 2014 has offered a unique opportunity to investigate the chemical composition and color of medieval glasses. This impressive corpus, covering a total surface of 660m$^2$, was created in a record time of a few years. The glasses from ten selected panels were analyzed using non-destructive and non-invasive techniques, with a specific consideration for the color of the glasses. Ion beam analyses performed at the New AGLAE facility enabled revealing that all ancient glasses are potash type glasses made from plant ashes, likely beech, in agreement with previous results on off-site panels. The multivariate analysis of major and minor elements demonstrates the presence of compositional clusters with a small variability suggesting the identification of bundles of glasses. The coloration of the glasses was measured by optical absorption spectroscopy, using a mobile spectrophotometer over the entire UV-visible-NIR energy range. The color palette is made of six colors assigned to typical medieval recipes. The chromophores of the different glasses are identified by combining the chemical composition, optical absorption spectroscopy and colorimetry. Colorless, yellow and purple glasses arise from the subtle redox equilibrium between manganese and iron. Their reduced usage shows their uncertain production. Blue glasses are colored by $Co^{2+}$ using saffre from the contemporary German mines, green glasses are colored by $Cu^{2+}$ and $Fe^{3+}$ using high concentrations of copper and red glasses are striated glass colored by metallic copper nano-particles. Glass matrix and chromophores form compositional clusters, which are spread among the panels of the four windows suggesting that the glazing of these four windows was run simultaneously by the same atelier using the same supply of glass.

# Keywords

Sainte-Chapelle, glass, color, PIXE, optical absorption, colorimetry, stained glass


# 1. Introduction

Archaeological and historical glasses provide unique information on the technological development and artistic sensitivities of past societies (Rehren and Freestone, 2015). Some foundations of our modern industrial societies may be found back in the medieval times and contained in the stone walls of the inherited cathedrals.(Musso, 2017; Panofsky, 1946) During the Middle Ages, the rise of Romanesque followed by Gothic architecture introduced a major change: the increasing size of openings in the walls, to be filled by stained glass windows, offered the opportunity to develop the art of glazing, where glass (translucent and colored glass) symbolized divine light. (Grodecki and Brisac, 1984; Lautier and Kurmann-Schwarz, 2010; Pallot-Frossard, 1998) In the mid 12$^{th}$ century, both Abbot Suger and the monk Theophilus praised the beauty and preciousness of colored glasses, which are similar to gems and would suggest the heavenly Jerusalem.(Grodecki, 1976; Hawthorne and Smith, 1979; Panofsky, 1946) The design and the glazing of larger windows might have been possible thanks to the technological improvement of glass production towards efficiency and high productivity. As a result, France has one of the largest heritage of medieval stained glass windows as revealed by its full inventory recently completed by the Corpus Vitrearum.

Over one century, the Gothic architectural revolution lead to one of the paroxysms of medieval stained glass art: the Sainte Chapelle in Paris, a UNESCO World Heritage Monument, and housing one of the most important corpus of medieval stained glass in the world, described in the first volume of the French Corpus Vitrearum's publications. Built between 1243 and 1248 to receive the relics of the Passion bought by King Louis IX (saint Louis), the exceptional glazing of the upper chapel forms walls of about 660m$^2$ of well preserved colored glasses.

The prolixity of the images which depict the stories of the Bible, almost reaches saturation of both colors and iconography.(Grodecki and Brisac, 1984) The hundreds of panels assembled in the windows were achieved within the construction time of the Sainte-Chapelle, thus in a span of only 6 years. This impressive efficiency suggests the collaboration of dozens of glaziers from different ateliers to complete the work in such a short time.(Grodecki and Brisac, 1984)

While the details of the work of Abbot Suger in the 12$^{th}$ century in the management of the construction and glazing of the abbey of Saint-Denis, France, are well documented (Panofsky, 1946), few original stained glass panels have been preserved. On the contrary, the Sainte-Chapelle in Paris is a uniquely well-preserved large corpus of stained glass, yet all archives about the construction and its glazing have been lost. Glass chemistry thus provides a precious insight in glass history, medieval glassmaking technology and glazing work organization. The study of the composition and the coloration of glasses is therefore an essential step in our knowledge of this material, its fabrication, and use in medieval times. Yet these glasses remain largely under-studied for only a few panels could be submitted to chemical analysis so far. To our knowledge, the only available chemical composition data published were obtained on panels removed from the building and belonging to museum collections.(Lagabrielle and Velde, 2005; Verita et al., 2005) This previous work lead to hypotheses suggesting that the glass used for glazing the windows was provided from two different regions of France: Ile-de-France and Normandy. However, these studies were restricted to a few glass samples and to a limited number of chemical elements. The opportunity of the restoration in 2011-2014 of the northern stained glass windows granted access to ten panels from windows 107, 109, 111, ad 113 for non-destructive chemical, spectroscopic and colorimetric characterization providing for the first time a large scale investigation of these glasses.

The chemical composition was obtained on 110 glasses from the ten panels by ion-beam analytical (IBA) methods, which allows the characterization of a large set of 35 major and trace chemical elements in a single acquisition.(Calligaro, 2008; Fleming and Swann, 1987; Hunault et al., 2017a; Kuisma-Kursula, 2000; Van Wersch et al., 2016; Vilarigues et al., 2019; Vilarigues and da Silva, 2004) The colors of the five panels of windows 111 and 113 were also investigated by optical

absorption spectroscopy using a portable optical spectrometer developed for contactless measurements(Hunault et al., 2016b). The glasses were studied after their restoration, thus allowing the reduction of the effect of surface deposit on the measurements. The handling of the complete panels allowed us to select the significant glasses to be analyzed from aesthetical, historical and chemical points of view.

We first report the chemical composition study of the glass matrix and its interpretation in terms of origin and glass recipes based on a multivariate analysis. We discuss the variability and dispersion of element concentration as a proxy of the glasshouse provenance. Then we describe the recipe of each glass color. Colorless, purple and yellow colors are first described together as they arise from subtle redox equilibria between iron and manganese ions as found in the monk Theophilus' treatise (Royce-Roll, 1994; Schreurs and Brill, 1984; Sellner et al., 1979; Theophilus, 1847). Blue, green and red colors are obtained by the addition of cobalt or copper. The sources for these elements are inferred and discussed.

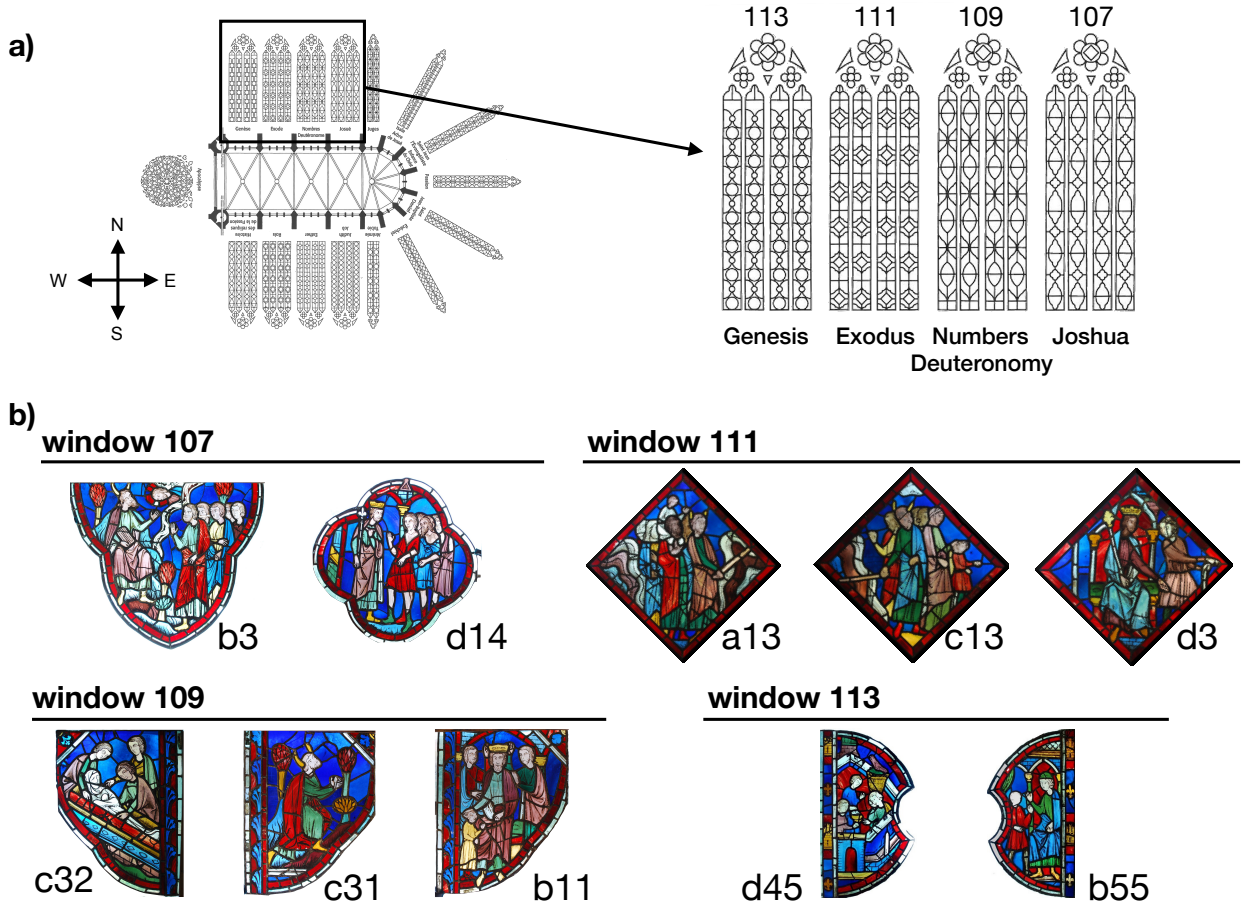



**Figure 1:** *a) The four windows restored in 2011-2014 and their location in the Sainte-Chapelle in Paris. b) The 10 analyzed panels.*

# 2. Methods

## 2.1. Historical identification of the glasses

The 15.5m-high windows of the nave, composed of thin lancets and crowned by small roses, were assembled from hundreds of small panels, covering a total surface of 660m$^2$. The careful study of the windows by art historians both in the 1950's and during the last restoration revealed that most of the glasses date from the 13$^{th}$ century,(Aubert et al., 1959; Grodecki and Brisac, 1984) thus providing an exceptional corpus of glasses testifying of the medieval glassmaking techniques. , The windows of the nave follow a complex iconographic program.(Aubert et al., 1959) The style of these stained glass windows is characterized by a simplification of the lines tending toward elegance. The color palette used is composed of red, blue, purple, green, yellow and colorless glass, the red and blue colors dominating the overall effect created by this colorful pattern. The

stained glass windows of the nave are attributed to three glazing ateliers based on the differences between the style of the painting.(Grodecki and Brisac, 1984)
Over centuries, they underwent several modifications, including the removal of numerous panels located in the lower part of the windows at the end of the 18$^{th}$ century and the beginning of the 19$^{th}$ century, when the building was used to accommodate the archives.(Grodecki and Brisac, 1984; Loisel, 2020) Some panels have been lost, while others are now in museum collections in France, Great-Britain and the USA.(Smith, 2015) An important restoration campaign decided by King Louis-Philippe in 1837 and undertaken between 1848 and 1855 resulted in the completion of the stained glass windows, by the means of new stained glass panels carefully imitating the remaining medieval ones.(Aubert et al., 1959)
The ten studied panels were observed by naked eye to achieve a critical identification of each glass pieces. The dating was achieved using several criteria: color, marks of blowing technique, irregularities, relative thickness variations, cutting pattern of the edges when visible, alterations and eventually the paintings on the glasses. It enabled to distinguish original glasses from the 13$^{th}$ century and more recent glasses introduced during the successive restoration campaigns.
During the restoration of 2011-2014, ten panels from the North side, the windows of Joshua, (window 107), Numbers and Deuteronomy (w. 109), Exodus (w. 111) and Genesis (w. 113) (Figure 1) were studied. According to stylistic analyses these four windows were glazed by the same artist from the main glazing atelier.(Grodecki and Brisac, 1984)

## 2.2. PIXE-PIGE chemical composition analysis

A total of 110 glasses were analyzed by Particle Induced X-ray Emission and Particle Induced Gamma Emission (PIXE and PIGE) techniques at the new AGLAE facility of the C2RMF in the Louvre (Paris, France).(Pichon et al., 2014) These non-destructive analyses were performed directly on the panels without sampling or removing the glass pieces. The repartition of the analyzed samples between the windows and the colors is given in supporting information (SI). PIXE and PIGE analyses were performed simultaneously. PIXE analysis was performed using four SDD detectors: the first one was dedicated to the analysis of low Z elements (10<Z<29) and a helium flux was used to reduce the absorption of incident and remitted beams by air; the three other SDD detectors were dedicated to high Z elements (Z>26) and an aluminum filter (50$\mu$m-thick) was placed in front of the detector in order to absorb the low energy X-rays. One HPGe detector was used for PIGE measurements. The incident proton beam was 3 MeV with an intensity of 3 to 4 nA. The chemical composition was averaged over an analyzed area of 1000$\mu$mx1000$\mu$m, using a 50$\mu$m-diameter beam. For each glass sample, three measurements were performed at different points. The obtained compositions correspond to the mean composition of all the analyzed area. The analyses were performed on the inner side of the panels, less altered, after cleaning the analyzed area with a water-ethanol solution. The PIXE spectra were extracted using GUPIX software combined with TRAUPIXE software developed at AGLAE(Pichon et al., 2015), assuming that analyzed zones were homogeneous and that all elements were present as oxides. The geochemical diorite DR-N sample and Brill glasses were used as reference material to calibrate the PIGE data and control PIXE results. The compositions given in this paper result from the combination of PIXE data and the sodium content obtained by PIGE.
Data were analyzed using the R software. Hierarchical cluster analysis (HCA) was performed after renormalization using Ward's method and Euclidean distances (see SI). This data analysis tool has been used previously in several studies of ancient glasses to compare glass compositions.(Cox and Gillies, 1986; Kunicki-Goldfinger et al., 2000; Schalm et al., 2007)

## 2.3. Optical absorption spectroscopy

The optical absorption spectroscopy measurements were performed in parallel to the chemical analysis on the same glass pieces. We used a mobile setup described elsewhere,(Hunault et al., 2016b) which enabled to measure optical absorption spectra in transmission over the entire UV-visible-NIR energy range (350-2500 nm). The beam size on the sample was smaller than 1 mm$^2$ and enabled to select a precise spot of analysis, free from alteration and paint.

Colorimetric analyses were achieved by computing the CIE L*a*b* values (unit less) in the colorimetric system defined in 1976 by the International Commission on Illumination. The colorimetric CIE L*a*b* values were calculated using D65 illuminant and CIE 1931 2° observer. L* describes the luminosity of the color (0: black; 100: white) and a* and b* describes the color hue: a* varies from -120 (green) to 120 (red) and b* varies from -120 (blue) to 120 (yellow), the higher a* and b* in absolute value, the more saturated the color.

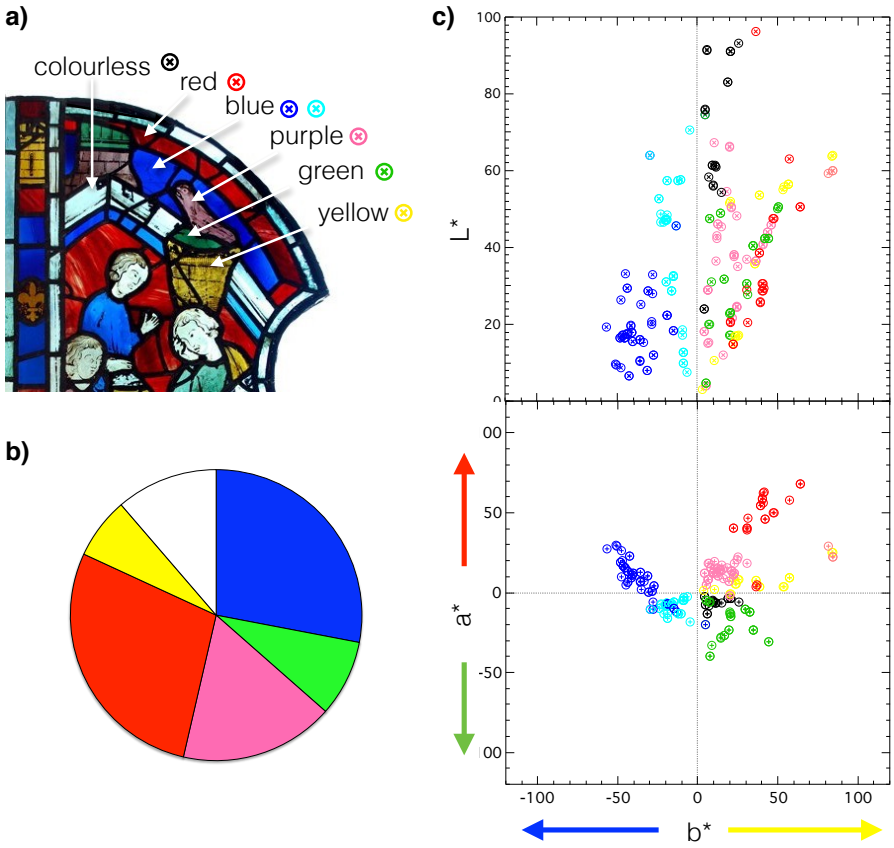



**Figure 2:** *a) Detail of the panel d45 (w. 113) and identification of the colors; b) Average glass surface fraction per color obtained for the ten panels of this study; c) CIE L*a*b* parameters obtained from optical absorption spectroscopy.*

# 3. Results and interpretations

## 3.1. Dating of the investigated panels

The ten panels of windows 107, 109, 111 and 113 that have been analyzed by portable optical absorption spectroscopy and PIXE-PIGE analysis are presented in Figure 1 and the corresponding restoration charts provided in Supporting information (SI) confirm that the majority of the glasses were original. The artistic and material quality of these windows is well preserved, despite the fact that these 13$^{th}$ century glasses have been altered by the atmosphere and air (Godoi et al., 2006; Bernardi et al., 2013). This study focuses on the original glasses from the 13$^{th}$ century representative of the different colors present in the four windows.

## 3.2. The color palette

Medieval stained glass windows are well known for the diversity of their colors. The colors of the glasses are named according to the usual terminology used by art historians: yellow, purple, red, blue, green, and colorless glasses (Figure 2a). This color distinction will be used hereinafter to report and discuss the chemical composition, spectroscopic and colorimetric data. By “colorless” we refer to glass that is not remarkably colored, either with a residual “natural” color or decolorized

by the addition of specific chemical elements. Other authors use the word “white” instead of “colorless” (Bidegaray et al., 2020; Gliozzo, 2016; Jackson, 2005).
Figure 2b shows the fraction of glazed surfaces of each color averaged by image analysis using GIMP software, over the ten studied panels. Blue and red glasses are the dominating colors in terms of surface, which confirms the general blue-and-red visual impression created by these stained glass windows. Based on the estimate of the total surface of 660 $m^2$ of the glazing of the nave windows, this gives a surface of 185 $m^2$ for red and blue glasses and 110 $m^2$ for purple glasses. Other colors correspond to a more limited surface: 70 $m^2$ for colorless glass and 60 and 45 $m^2$ for green and yellow glasses, respectively.

The 1976 CIELAB color space coordinates (L*, a*, b*) provide a way to quantify the variability of the hue and luminance. Figure 2c presents the colorimetric parameters of the studied glasses for each color. Red glass is the most saturated color with high absolute a* and b* values. The blue glasses split into two groups, according to a* value: negative or positive for the greenish or reddish hue, respectively. These two colors span over a wide range of a* and b* values together with green glasses and yellow glasses. Purple and colorless glasses consist of a more reduced range of a* and b* values. The glasses cover the entire range of luminance values L*, and we can note that blue glasses are generally darker (lower L* value) than colorless glasses (higher L* value).
Color results from the overall absorption of light by the material, thus not only the chromophores, added to the glass to give its color but also surface alteration or paint influence the color. Although we took special care to analyze glasses with minimal influence of alteration and paint, the variation in luminance L* value may reflect the influence from both factors.
In the followings, we will use the color distinction described above to report and discuss the chemical composition data.

## 3.3. Composition of the glass matrix

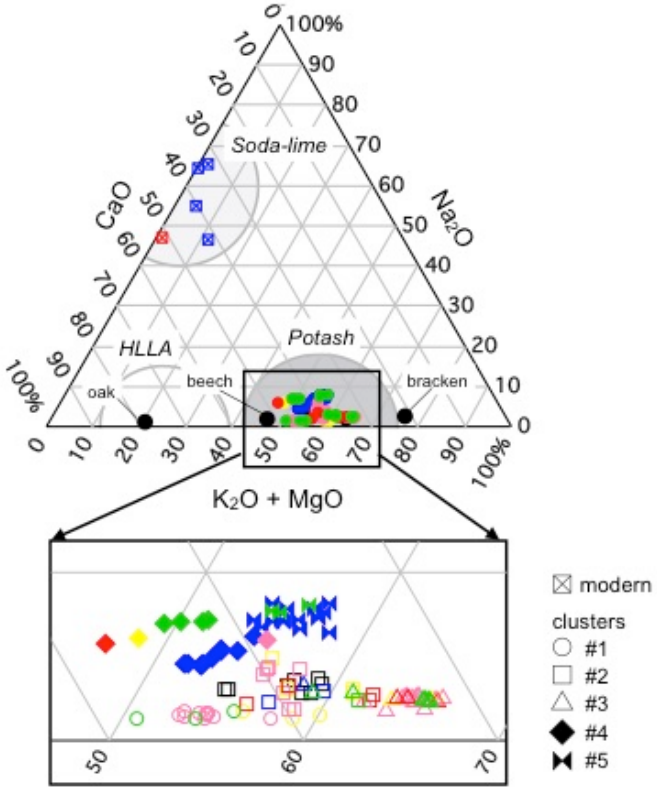



**Figure 3:** *Ternary diagram $Na_2O$-$K_2O$+MgO-CaO showing the relative concentrations of four major elements characteristic from the type of flux used to produce the medieval glasses of the Sainte-Chapelle in Paris. The color of the markers represents the color of the glass in agreement with the colorimetry analysis (see main text). The inset shows the distinction between the five clusters of compositions found within the “potash” group using hierarchical cluster analysis (see main text);*

*Chemical compositions of glasses obtained from specific ashes from ref.(Jackson and Smedley, 2004), are indicated (black full circles).*

### 3.3.1. Medieval recipe: wood-ash glasses

- Glass type

Medieval glasses were obtained by melting together silica from sand and a flux. The chemical composition of the resulting glass reveals to some extent the nature of the flux used. Compositions of ancient glasses from the 12$^{th}$-16$^{th}$ centuries have been classified by several authors (Adlington and Freestone, 2017; Gratuze, 2013; Kunicki-Goldfinger et al., 2014; Schalm et al., 2004) into:
- “Soda-lime” glasses including natron glasses and halophilic plant ash glasses;
- "Potash" glasses: potash-lime silicate glasses obtained using plant ashes;
- “High Lime-Low Alkali” (HLLA) glasses: these glasses, obtained using plant ashes, contain more calcium than alkaline elements.

The complete set of chemical concentrations of all elements analyzed by PIXE-PIGE at AGLAE can be found as Supporting Information. Figure 3 presents the ternary diagram of the relative concentrations of the four major elements characteristic from the type of flux used to produce the glasses: $Na_2O$, $K_2O$, CaO and MgO. Potassium and magnesium are summed together as both come from plant ashes that could have been used as a source of flux.(Jackson et al., 2005; Jackson and Smedley, 2008; Smedley and Jackson, 2002) On the ternary diagram, we have represented the areas for each glass type.
Among the 110 analyzed glasses, five glasses originally identified as ancient glasses, were found to be soda-lime glasses with their $Na_2O$ content higher than 11wt%. These glasses were identified as restorations from the 19$^{th}$ century. This is supported by their low magnesium and phosphorous contents, both elements that indicate the use of plant ashes (Jackson et al., 2005; Jackson and Smedley, 2008; Smedley and Jackson, 2002) and by the low impurity level resulting from the use of relatively pure raw materials. *In the following, these glasses will be ignored*.
All the 105 other glasses from the ten analyzed panels from the Sainte-Chapelle in Paris belong to the “potash” type area and show high potassium oxide and lime contents (Figure 4a). The high magnesia and phosphate contents further confirm the use of wood ashes (Figure 4b and Figure S5). We note that the glasses from the Sainte-Chapelle in Paris belong to the category of low-lime high-magnesia content (LLHM) as distinguished by Adlington et al. (Adlington et al., 2019) (Figure S5). The phosphate content (in the 3-5wt.% range) and the sodium oxide content are relatively high compared to other plant-ash medieval glasses (Figure S5). Altogether, the composition of the glasses from the Sainte-Chapelle in Paris agrees with the general pattern found for North Western France glasses as reviewed by Adlington et al. (Figure S5). Additionally we note that the chemical composition of the 13$^{th}$ century glasses of the Sainte-Chapelle is similar to several other medieval glasses in terms of potassium oxide, lime, magnesia and phosphate contents: i) earlier glass compositions from the end of the 8$^{th}$ century eastern France.(Van Wersch et al., 2016); ii) 12$^{th}$ century potash glasses from York Minster, UK.(Cox and Gillies, 1986) iii) medieval German wood-ash glasses from before 1400.(Wedepohl and Simon, 2010) and iv) later 15$^{th}$ century Belgian glasses.(Schalm et al., 2007)

The use of wood ashes as flux agrees with ancient treaties.(Smedley and Jackson, 2002) The fluxing properties of the ashes arise from their alkali and alkaline-earth contents. Depending of the nature of the ashes used in the glass recipe, various chemical compositions were obtained. Despite similar potassium oxide and lime compositions (Figure 4a), the ternary diagram highlights the horizontal spread of the data along the CaO-$K_2O$+MgO joint as well as several distinct $Na_2O$ contents, which can be markers of glass recipe variations.

- The recipe

Experimental studies on the relation between the nature of the ashes and the resulting glass composition are difficult as the composition of wood ashes depends on many factors. Yet previous

investigations have brought precious information on the influence of the type of ashes on the final glass composition. Jackson et al. compared glasses obtained from beech, oak and bracken ashes.(Jackson and Smedley, 2004) They showed that beech ashes give close $K_2O$ and CaO contents and high phosphate content; oak ashes give high CaO and low $K_2O$ contents and low phosphate content; and bracken ashes give high $K_2O$ and low CaO contents and a medium phosphate content. These compositions are reported in Figures 3 and 4 and S5 for comparison with the present data. Figure 3 clearly suggests the dominant use of beech ashes potentially mixed with bracken ashes. (Jackson and Smedley, 2008, 2004; Smedley and Jackson, 2002) Stern and Geber investigated the chemical composition of glasses made from two different recipes:(Stern and Gerber, 2004) i) beech ashes and sand and ii) leached beech ashes, potash extract and sand. The "potash"-type chemical composition found in the present study with close $K_2O$ and CaO contents is close to the second recipe suggesting the additional use of potash extract obtained from leached ashes. This is partly in contradiction with the results of the study of Jackson et al. who used unpurified ashes. However, the second recipe from Stern and Geber's study does not account for the high phosphate content. The addition of bracken ashes may explain the observed high phosphate content. Altogether, the chemical composition of the glasses suggests that the glasshouses, which provided the glasses for the Sainte-Chapelle, used beech ashes, possibly mixed with bracken ashes, conforming to the recipe found in the monk Theophilus' treatise.(Hawthorne and Smith, 1979)

The glasses from the Sainte-Chapelle in Paris appear to have among the highest silica content in Medieval Europe, with an average 57.6 wt% $SiO_2$ (Figure 3b and see Table I), which is higher than the values reported in other medieval "potash"-type glasses (Calligaro, 2008; Freestone, 1992; Hunault et al., 2016a). In their experimental work, Smedley et al. (Smedley et al., 1998), discussed the weight ratios between ashes and sand according to the monk Theophilus's treaties, in relation with the melting temperature of the glass as well as its durability. The higher the ash content, the lower the melting temperature and the easier the completion of the melt yet resulting in a less durable final glass. At fixed sand-to-ash ratio, depending on the flux chemical composition, the resulting melting and working properties of the glass may differ. Vice versa, the sand-to-ash ratio might have been adjusted depending on the flux composition to obtain similar melting and working properties of the glass.(Hunault et al., 2017b) Here, the relatively high silica content would suggest the use of high quality, high durability glass in accordance with the final purpose of the Sainte-Chapelle building to host the Passion relics.

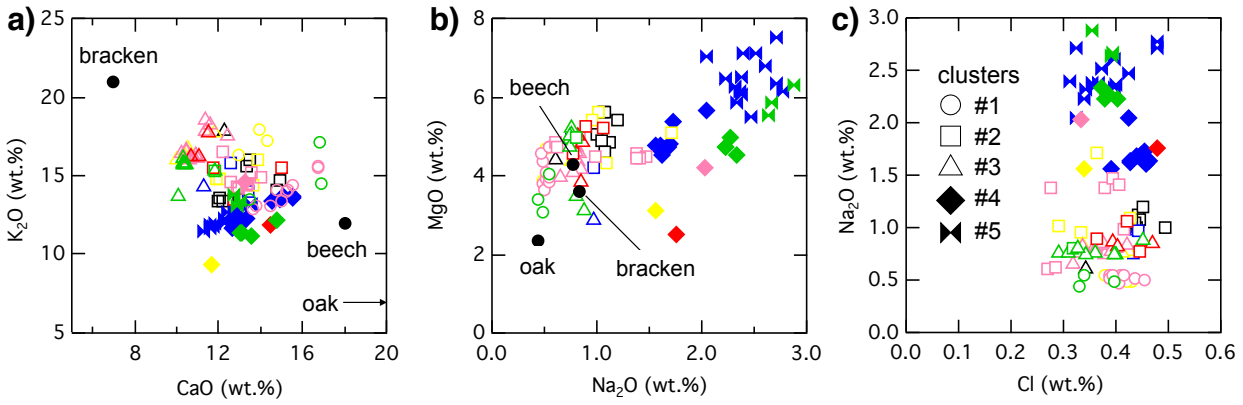



**Figure 4:** *Chemical compositions analyzed by PIXE-PIGE at the New AGLAE facility a) $K_2O$ vs CaO, b) MgO vs $Na_2O$ and c) $Na_2O$ vs Cl. Markers correspond to the clusters and colors to the glass colors. Error bars are of the size of the markers.*

- Sodium-enriched potash glasses

A number of "potash" type glasses are enriched in sodium (>1.5wt.% $Na_2O$) (Figure 3 and Figure 4b). A majority of these glasses corresponds to blue glasses, other to some green glasses, and a few correspond to other colors. The glasses are enriched in both sodium and magnesium, which discards a possible recycling of natron-based glasses that do not contain magnesium.(Phelps et al., 2016; Tite et al., 2006) There is no correlation between the chlorine and the sodium contents

(Figure 4c): the Cl content is constant in the 0.3-0.5% range, while the $Na_2O$ content varies by a factor of 6. This supports that salt was not used similarly to other medieval Belgian glasses.(Schalm et al., 2007) Furthermore, none of the laboratory synthesized wood ash glasses contain sodium up to similar ranges as observed here (Figure 4b).(Jackson et al., 2005; Jackson and Smedley, 2008; Smedley and Jackson, 2002; Stern and Gerber, 2004) It is therefore not clear whether this sodium increase is related to the nature of the wood ashes.

Is the sodium-enrichment a marker from a specific geographical provenance? Sodium-enriched glasses have been found in various medieval glasses (Adlington et al., 2019), such as panels from other windows of the Sainte-Chapelle in Paris (Lagabrielle and Velde, 2005; Verita et al., 2005), from the abbey of Saint-Denis, France (Calligaro, 2008), and from Westminster, UK and Cluny, France.(Freestone, 1992) Based on the comparison with the chemical composition of other French glasses from the same period and in particular the glasses from the cathedral of Rouen, France, previous authors have further hypothesized that the low $Na_2O$/MgO ratio glasses came from Ile-de-France, France and the high magnesium and sodium content glasses came from Normandy, France.

What is the origin of this sodium-enrichment? Little inferences have been made so far. We may suggest two possibilities: i) the recycling of ancient soda-type glasses as was available in Europe until the 12$^{th}$ century (Cox and Gillies, 1986) in low proportions such as significant characteristic impurities are not detected (Bidegaray and Pollard, 2018) or ii) use of sodium-rich seaweed ashes in addition to wood ashes (Adlington et al., 2019; Tite et al., 2006; Wedepohl et al., 2011a).

Although the majority of blue glasses found in this study would suggest a specific trade from a distinct glasshouse for this color, or a specific recipe related to the cobalt source(Bidegaray and Pollard, 2018), previous data from other panels from the Sainte-Chapelle, revealed the presence of glasses of similar sodium content with other colors (see Figure S10 in SI). The observation of a similar composition pattern among the different windows suggests that the different glaziers used glass from the same stock.

### 3.3.2. Variability of major and trace elements: different glasshouses?

The obtained relatively close chemical compositions can suggest a common origin of the glasses. However, some subtle variations are observed. These variations could account for different production origins or variability in the production of one same glasshouse. How close are the chemical compositions of glasses produced in the same glasshouse?

Several factors influence the chemical composition of Medieval glasses, independently of the use of coloring additives. The variability within one glasshouse can be separated into “natural” and “behavioral” variations, related to the raw material chemistry and glassmaking techniques, respectively.(Freestone et al., 2009; Jackson et al., 2005) Another factor influencing the chemical composition variation is the time scale over which the compared glasses have been produced in one glasshouse. Indeed, the incidence of “behavioral” and “natural” variations are more likely to be effective over weeks, months and even years than over one single day since glass pots were used over several days.(Freestone et al., 2009) In a recent work, we have estimated the “daily variation” criterion based on the comparison of the chemical composition of four different glasses assembled together in one pane of glass, guarantying that these glasses originated from glass pots operated on the same day.(Hunault et al., 2017a) This criterion corresponds to the variation of glass composition between different glass pots prepared in the same time frame in the same glasshouse. The time unit of one day is supported by the time reference found in Theophilus’ treatise, which states that glass could be melted overnight and that it would take only a few hours to observe color changes.(Hawthorne and Smith, 1979; Smedley et al., 1998) We may consider this variation as a reference minimum variation of the production of a glass glasshouse.

This “daily variability” criterion can be compared to the composition variation (relative standard deviation) calculated for the major components of all the analyzed ancient glasses of the Sainte-Chapelle in Paris (Table I). We find that the composition variation of the ancient glasses is at least twice larger (for $Al_2O_3$ and CaO) than the “daily variability”. This agrees with the fact that all the

glasses could not be produced over one day in one glasshouse. Hence, the larger variability in the chemical composition can be assigned to both "natural variability" and "behavioral variability" across time within the same glasshouse or to different provenances.

Yet according to the ternary and binary diagrams (Figure 3 and Figure 4), it is tempting to define clusters of data with close chemical compositions. To define clusters of glasses based on more than two or three chemical composition variables, we used hierarchical cluster analysis (HCA) considering 13 major and trace elements corresponding to the raw materials of the glass: Si, Na, K, Ca, Mg, Al, Cl, P, Ti, Rb, Sr, Zr and Ba as oxides. These elements describe the glass batch independently from coloring chemical elements and other associated elements. Iron and manganese are excluded from the HCA because their content is also influenced by the addition of coloring ores (see below).

**Table 1 :** Average values and relative standard deviation (compositional variability) of chemical composition for the ancient glass corpus for each cluster.

| | $Na_2O$ | MgO | $Al_2O_3$ | $SiO_2$ | $P_2O_5$ | $K_2O$ | CaO |
|---|---|---|---|---|---|---|---|
| | Daily glasshouse variability according to Hunault et al. 2017 | | | | | | |
| *Rel. SD (%)* | *14* | *4* | *6* | *1* | *3* | *4* | *7* |
| | All ancient glasses (N=105) | | | | | | |
| Av. (wt%) | 1.24 | 4.84 | 1.95 | 57.0 | 3.97 | 14.5 | 12.7 |
| *Rel. SD (%)* | *57* | *19* | *11* | *4* | *14* | *13* | *13* |
| | Cluster #1 (N=16) | | | | | | |
| Av. (wt%) | 0.5 | 4.0 | 2.2 | 54.8 | 4.9 | 14.8 | 15.0 |
| *Rel. SD (%)* | *6.5* | *12* | *6.0* | *4.5* | *3.5* | *11.* | *8.6* |
| | Cluster #2 (N=26) | | | | | | |
| Av. (wt%) | 1.0 | 4.9 | 1.8 | 57.3 | 3.7 | 14.7 | 13 |
| *Rel. SD (%)* | *25* | *8.7* | *11* | *2.9* | *15* | *6.1* | *7.3* |
| | Cluster #3 (N=30) | | | | | | |
| Av. (wt%) | 0.79 | 4.5 | 1.8 | 58.3 | 3.6 | 16.4 | 10.9 |
| *Rel. SD (%)* | *8.5* | *13* | *4.8* | *2.2* | *5.9* | *6.6* | *6.0* |
| | Cluster #4 (N=16) | | | | | | |
| Av. (wt%) | 1.9 | 4.5 | 1.9 | 57.0 | 4.2 | 12.4 | 13.8 |
| *Rel. SD (%)* | *15* | *17* | *6.5* | *5.2* | *8.3* | *11* | *8.3* |
| | Cluster #5 (N=17) | | | | | | |
| Av. (wt%) | 2.5 | 6.4 | 2.1 | 56.0 | 4.0 | 12.5 | 12.4 |
| *Rel. SD (%)* | *8.8* | *8.9* | *6.6* | *2.9* | *6.5* | *5.3* | *5.3* |

The obtained dendrogram and the inertia plot are provided in SI and the significance of the chosen method is further discussed in the SI and below. The dendrogram first splits into two branches that mainly correspond to the high and low $Na_2O$ contents respectively and accordingly to most of the blue glasses and the others. This agrees with the trend observed in the ternary diagram (Figure 3) and in Figure 4, where two main groups of glasses are separated according to their $Na_2O$ content. Following the inertia plot we define five significant clusters. The clusters are further described in the SI. These clusters, based on these 13 major and trace elements, are reported in all plots as different markers, and agree fairly with the groups of data qualitatively observed in the ternary diagram and the other binary diagrams (Figure 3 and Figure 4 and hereinafter). In Table I, the means and relative standard deviations for each cluster are given. We find that the chemical composition variations for each cluster are very close to the "daily variability". The narrowest

variations are found for cluster #5. Then cluster #3, though the largest one (30 glasses), shows also a low variability.

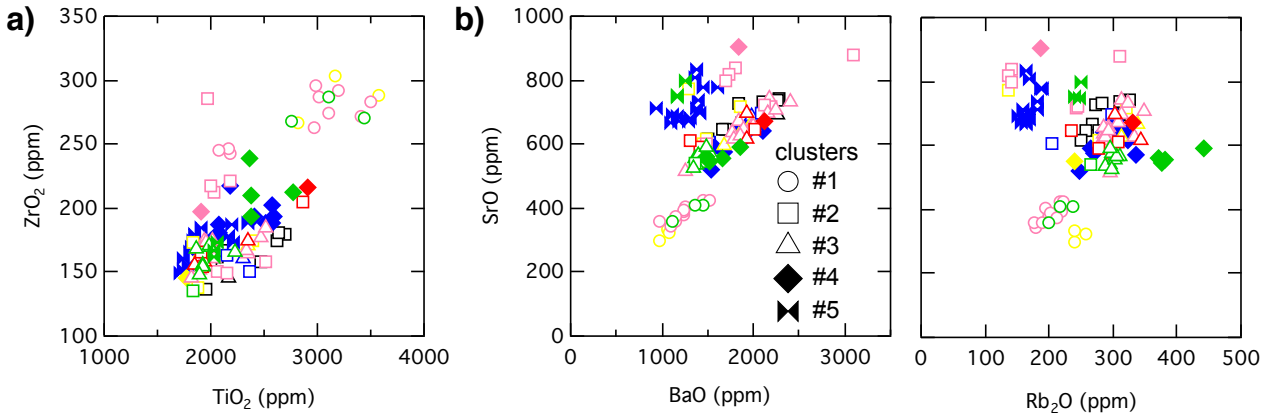



**Figure 5:** *Chemical compositions analyzed by PIXE-PIGE at the New AGLAE facility a) $ZrO_2$ vs $TiO_2$; b) SrO vs. BaO and $Rb_2O$ and ; Markers correspond to the clusters. Error bars are of the size of the markers*

In the HCA approach we have included some minor elements. Are the clusters significant regarding these components? Minor elements arising from raw material impurities might be markers of distinct sources and may help to further distinguish or confirm the common origin of glasses. Several authors have observed correlations between titanium and zirconium from heavy minerals (Neri et al., 2019; Rehren and Brüggler, 2015; Schibille et al., 2016; Wedepohl et al., 2011a) or strontium and rubidium from feldspars (Adlington and Freestone, 2017) and assigned them to markers of the raw materials used for making the glass. Figure 5a and Figure 5b show respectively the Ti and Zr and the Sr and Rb and Ba oxide contents. Cluster #1 forms a distinct group regarding these five elements. Cluster #5 forms also a distinct group of glasses regarding the Sr, Ba and Rb oxide contents. Clusters #2, #3 and #4 show similar Ti, Zr, Sr, Ba and Rb oxide contents (Figure 5). Very close trace element contents may suggest a common glasshouse origin. Yet the cluster #4 is quite distinct in terms of sodium oxide and magnesia contents. This observation shines light on the difficulty to distinguish origins based on chemical composition: bundles of glasses with similar trace element contents could be fortuitous, while important variations in major elements could arise from a recipe variation in the glasshouse.

Although, the definition of the clusters is dependent on the method used (see SI), we have shown that we can build significantly large clusters of glasses with low variability of major element composition and corresponding to distinct trace element compositions. It suggests that these sub-groups of glasses could, for most of the assigned samples, correspond to distinct bundles of glasses.

## 3.4. Origin of the colors

### 3.4.1. Colorless, purple and yellow glasses

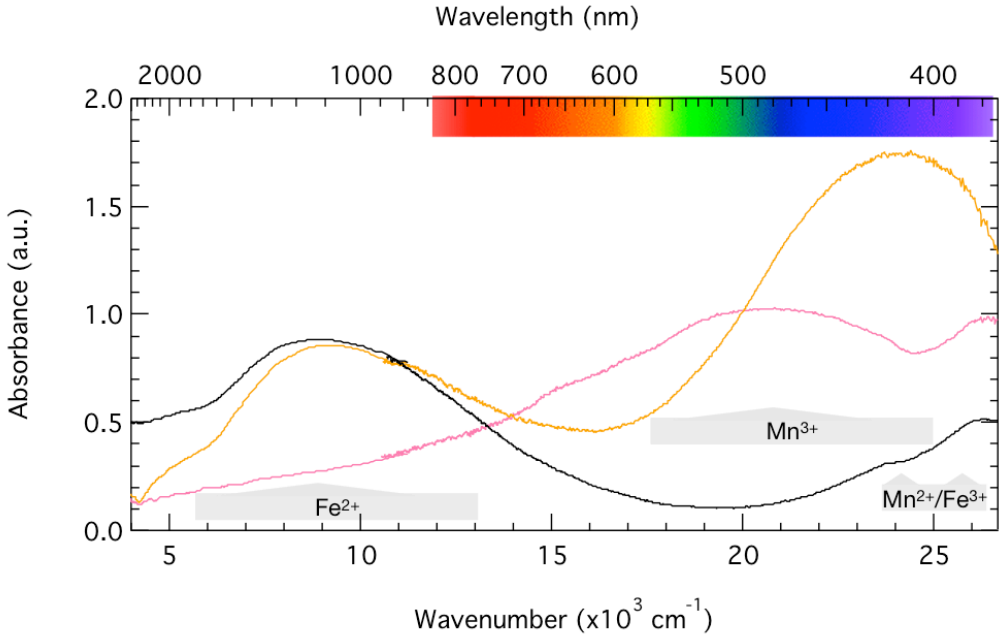



**Figure 6:** ***Optical absorption spectra of typical colorless, purple, and yellow glasses (with respective line color: pink, black and yellow)*** **and assignment of the absorption bands.**

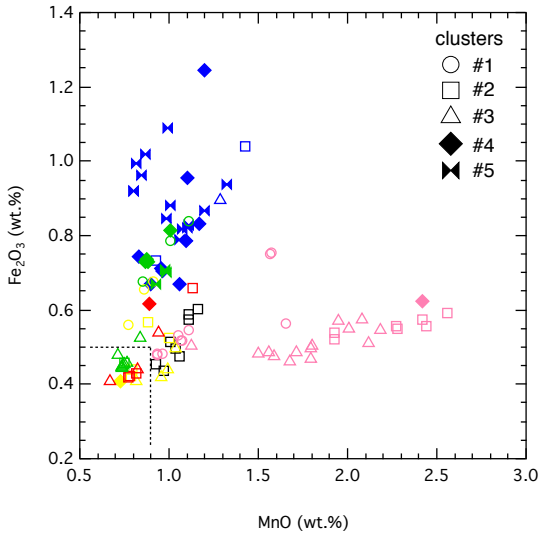



**Figure 7:** ***: Iron vs. manganese concentrations as total oxides with highlight on the colorless, purple and yellow glasses. Markers correspond to the clusters, color of the markers indicates the glass color, error bars are of the size of the markers.***

We first consider the colorless, purple and yellow glasses. The optical absorption spectra (Figure 6) correspond to glass samples assigned to cluster #2. The absorption bands are identified and reveal that these glasses are all colored (or uncolored) by their respective iron and manganese contents (Table II) and corresponding redox states ($Fe^{2+}/Fe^{3+}$ and $Mn^{2+}/Mn^{3+}$). These three colors represent roughly only one third of the glazed surface (Figure 2b). This agrees with the relative difficulty and uncertainty to obtain these colors (Royce-Roll, 1994;

Schreurs and Brill, 1984; Sellner et al., 1979), which mainly result from a subtle balance between the Fe/Mn ratio and the $Fe^{2+}/Fe^{3+}$ and $Mn^{2+}/Mn^{3+}$ relative amounts during glassmaking.

**Table II: Average iron and manganese contents (in wt.% ± standard deviation) of the colorless, purple and yellow glasses, independently of the cluster.**

| Color | $Fe_2O_3$ | MnO |
|---|---|---|
| Colorless | 0.52±0.06 | 1.0±0.08 |
| Purple | 0.53±0.07 | 1.65±0.5 |
| Yellow | 0.50±0.10 | 0.87±0.1 |

- Colorless glass

In the panels, colorless glasses are used for character's faces, walls, water, and folds. Colorless glasses correspond to glasses with no strong perceptible color hue, which translates in terms of CIE L*a*b* color coordinates as a* and b* being close to the center of the diagram (a*=0 and b*=0) and often the luminance L* being higher than 50 (Figure 2c). These values agrees with other reported values for colorless glasses.(Bidegaray et al., 2020, 2019; Capobianco et al., 2019) Yet they show a greenish color (negative CIE a*). The optical absorption spectrum of a typical colorless glass (Figure 6) from the Sainte-Chapelle in Paris agrees with previously published data. (Bidegaray et al., 2020, 2019; Capobianco et al., 2019; Hunault et al., 2017a) The greenish color is due to $Fe^{2+}$ that gives a broad absorption band in the NIR centered at 9000$cm^{-1}$ (1100nm) (Figure 6) and absorbs the red, orange and yellow wavelengths more than the green and blue side of the light spectrum. In glass, iron is present as $Fe^{2+}$ and $Fe^{3+}$ in various relative amounts depending on the glass chemical composition and redox conditions of fabrication. To remove the green color, the most common process is to oxidize $Fe^{2+}$ into $Fe^{3+}$ by adding an oxidizer to the glass, such as manganese and antimony. Red, yellow and some green glasses show the lowest iron and manganese contents (Figure 7), which allows us to define the impurity level concentrations to <0.5wt.% as total $Fe_2O_3$ for iron and to <0.9wt.% as total MnO for manganese (dashed lines in Figure 7). In Antiquity and the middle ages, glassmakers were using manganese in an oxidized form, referred to as "glassmaker's soap".(Bidegaray et al., 2020; Bingham and Jackson, 2008; Gliozzo, 2016; Jackson, 2005) The use of antimony in the glasses of this study is dismissed by the very low concentrations found in these glasses (maximum 200ppm). The colorless glasses of the Sainte-Chapelle in Paris, all belong to cluster #2 (Figure S7), and their manganese content is systematically larger than the impurity level concentrations (Figure 7 and Table II), which suggests the use of the "glassmakers' soap".

- Purple glass

The optical absorption spectrum of purple glass from the Sainte-Chapelle agrees with typical spectra from $Mn^{3+}$ colored glass.(Bidegaray et al., 2019; Capobianco et al., 2019; Hunault et al., 2017a). Compared to the colourless glasses, we observe the disappearance of the absorption band of $Fe^{2+}$, and the presence of $Fe^{3+}$ and $Mn^{2+}$, which only give weak absorption bands in the blue and UV range (Figure 6). The addition of more oxidized manganese than iron results in all $Fe^{2+}$ being oxidized(Schreiber, 1986). The excess of $Mn^{3+}$ colors the glass in purple with a broad and intense absorption band around 20800 $cm^{-1}$ (480nm) (Figure 6). The color shift from colorless towards purplish hue is observed in the CIE L*a*b* diagram with a change from negative to positive a* parameter. The purple glasses exhibit a large variation in the luminance values, with some strongly absorbing glass pieces (low L* value).
Visually, we observe two main uses of purple glass: characters' complexion using light purple or colorless glass and robes and dresses using more intense or darker purple glass.
Figure 7 reveals two groups of purple glasses according to their Mn content: a first group with Mn content close to the impurity level and a second group with a clear increase of the total manganese content larger than the other colors (>1.5wt.%), while the iron content remains mainly constant around 0.5wt.% (Table II). We observe that all dark purple glasses have high manganese contents.

- Yellow glass

Yellow glasses were used for clothes, horns, and crowns. The CIE L*a*b* colorimetric coordinates spread in luminance L* and along the b* (yellow) direction as a* remains small and positive. They are bulk colored and show an optical absorption spectrum (Figure 6) with a broad absorption band centered at 9000cm$^{-1}$ (1100nm) assigned to the presence of $Fe^{2+}$ as in the colorless glasses. An additional intense band in the UV creates the absorption deep centered ca. 16000cm$^{-1}$ (625nm) resulting in the yellow color. The lack of efficiency of the optical spectrometer source at high energy is responsible for the drop of absorption in the UV range in the recorded data. The addition of a complementary UV light source can improve the sensitivity in this energy range of the spectrum(Capobianco et al., 2019). The observed spectra differ from the yellow glasses of the rose of the cathedral of Reims (France) in the relatively more intense $Fe^{2+}$ absorption band. (Capobianco et al., 2019) The bulk coloring, the dating of the glass and the optical absorption spectrum altogether converge with the exclusion of the use of yellow silver stain, a painting technique that appeared only at the end of the 13$^{th}$ century or at the very beginning of the 14$^{th}$ century.(Jembrih-Simbürger et al., 2002; Lautier and Sandron, 2008; Molina et al., 2013; Pérez-Villar et al., 2008) The chemical composition of the yellow glasses is close to that of the colorless glasses and prevents us from identifying without any ambiguity a specific coloring element. According to Figure 7, iron and manganese contents are among the lowest. There are little data in the literature about bulk medieval yellow glasses. The optical absorption spectrum is consistent with the coloring species being the ferric iron-sulfide chromophore similarly to amber glasses. Yet, the sulfur content does not show any significant pattern in relation with the yellow color (Figure S12). Specific reducing conditions as encountered in the elaboration of amber glasses could explain how such colors were obtained.(Paynter and Jackson, 2018; Schreurs and Brill, 1984) In his treatise, Theophilus' description of the making of yellow glass seems rather circumstantial.(Hawthorne and Smith, 1979) More detailed information can be found in the 18$^{th}$ century treatise of Georges Bontemps (Bontemps, 1868) who provided two recipes for bulk colored yellow glasses based on: i) a particular balance between iron and manganese concentrations or ii) the use of wood still containing sap. Altogether, it suggests that the color is obtained by several steps of melting and refining.

### 3.4.2. Blue glasses

As illustrated with panel c13 from window B111 (Figure 8a), we can distinguish two types of blue glass: light blue glass, used for clothes, walls and dark blue glass used mainly for the sky or background. This distinction can be further confirmed in terms of colorimetry (Figure 8b): dark blue glass pieces show luminance L* values all smaller than 40, while light blue glass pieces spread over the entire luminance range. Both types can also be distinguished in terms of color hue: while all blue glasses have a negative b* value in agreement with the blueish hue, the light blue glasses have a negative a* value, showing a green contribution to the color, while the dark blue glasses have a positive a* value revealing the red component of the color hue.

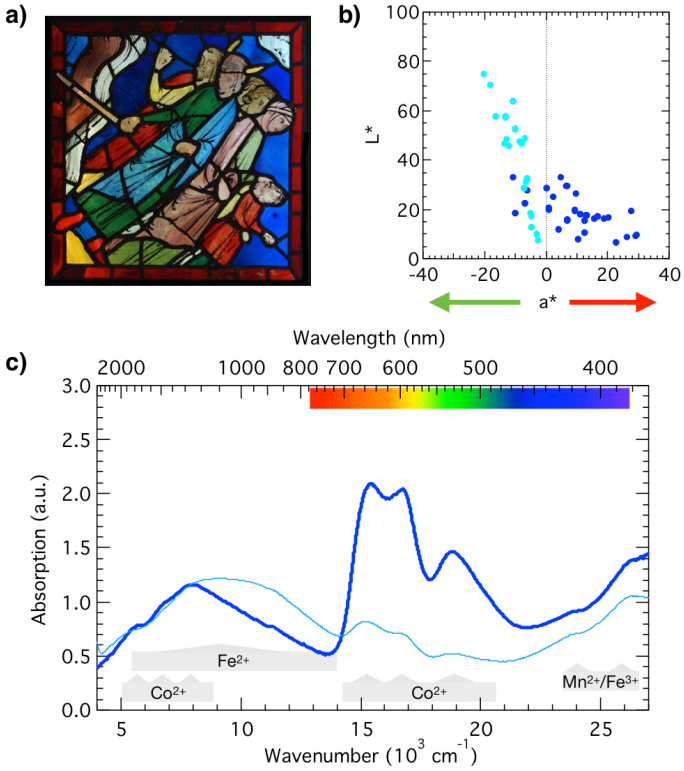



**Figure 8:** *a) Panel c13 (w. 111) showing the two types of blue glass; b) Colorimetric parameters L* vs. a*; c) Optical absorption spectra of typical dark blue glass and light blue glass and assignment of the absorption bands.*

Figure 8c presents a selection of two optical absorption spectra representative of the two types of 13$^{th}$ century blue glasses of the Sainte-Chapelle in Paris: light blue and dark blue. We observe the contribution of the two triplet absorption bands in the NIR range at 5500-8000 cm$^{-1}$ (1200-2000 nm) and the visible range at 15420, 16800 and 18800 cm$^{-1}$ (532, 595 and 650 nm) regions assigned to $Co^{2+}$ (Bamford, 1977; Hunault et al., 2016a, 2014) These visible range bands are more intense for dark blue glass than light blue glass. The chemical composition analyses (Figure 9) confirm that $Co^{2+}$ is the main coloring element in all blue glasses despite its relatively low concentration (maximum 1500ppm CoO). This is a result of its strong molar extinction coefficient.(Hunault et al., 2014) According to the Lambert-Beer law, the color intensity and darkness is proportional to the cobalt concentration assuming a constant glass thickness. Accordingly, we find that light blue glasses all correspond to low cobalt concentrations (Figure 9). The optical absorption spectra explain the color difference between the two types of blue: the $Co^{2+}$ absorption bands are relatively narrow, resulting in sharp absorption of the yellow and green wavelengths, while the blue and red wavelengths are not absorbed thus resulting in a positive a* parameter for dark blue glasses. In addition, we observe a broad absorption band between 7000 cm$^{-1}$ and 13000 cm$^{-1}$ (1428nm and 770nm) centered around 9000 cm$^{-1}$ (1100nm), superimposed on the near infrared absorption band of $Co^{2+}$. We can attribute this contribution to $Fe^{2+}$ similarly to the absorption band observed in the colorless glass.(Bingham and Jackson, 2008; Capobianco et al., 2019; Hunault et al., 2016a, 2017a) The contribution from the $Fe^{2+}$ band with respect to the $Co^{2+}$ bands is higher in the light blue glasses. The overlap with the relatively intense $Fe^{2+}$ absorption band results in a stronger absorption of the red wavelength and hence a dominant greenish-blueish hue (negative a*). The small absorption bands around 24000 cm$^{-1}$ (417nm) attest for the presence of $Mn^{2+}$ and $Fe^{3+}$.(Nelson and White, 1980; Vercamer et al., 2015) No significant increase in the Mn content is observed (average MnO content in blue glasses: 0.96±0.40 wt.%) suggesting that manganese arises only from the raw materials used for the glass (Figure 7).

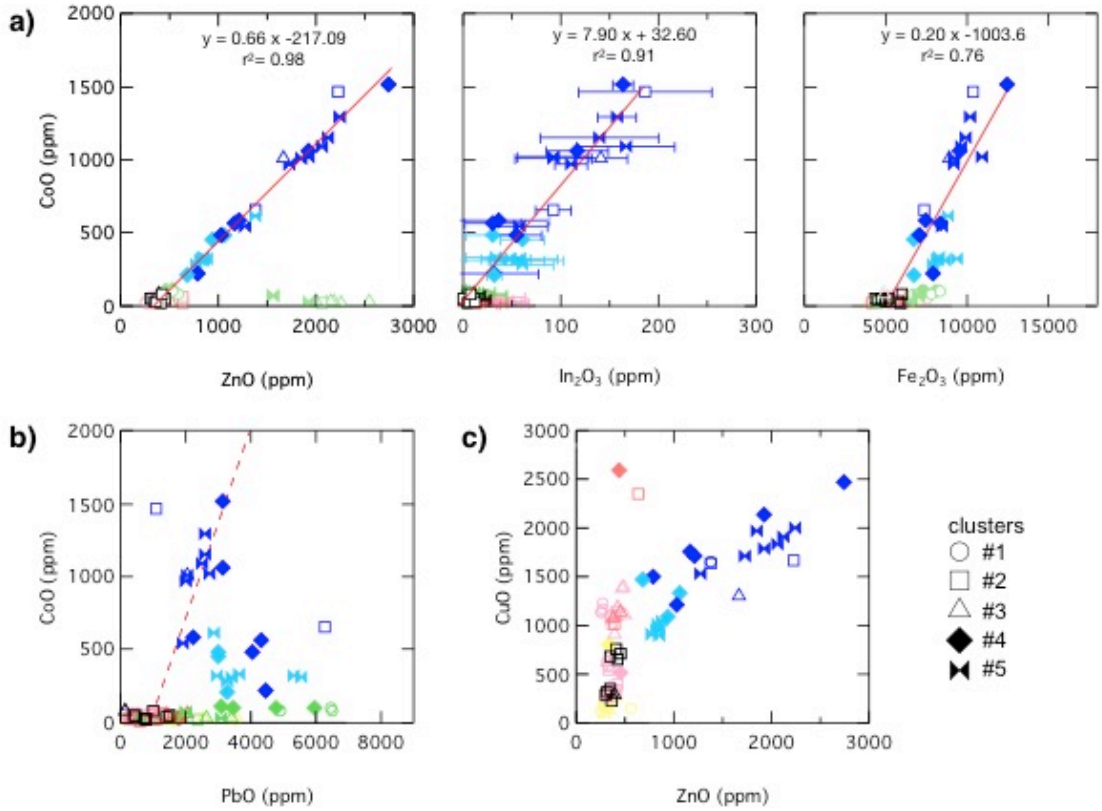



**Figure 9:** ***Chemical composition of the glasses obtained by PIXE at the new AGLAE facility in CoO v. a) ZnO, $In_2O_3$, $Fe_2O_3$ and b) CuO v. ZnO and c) CoO v. PbO. Unless indicated, error bars are of the size of the markers. Redlines indicate the linear regression fitting of the data for ancient colorless and blue glasses only (other colors excluded from the fit). Equations of the lines are given. The dotted line corresponds to a slope of 0.66 in agreement with the chemical composition of saffre.***

Blue glasses show clear correlations between cobalt and zinc and cobalt and indium contents (Figure 9a). These results agree with the sources of cobalt used in the 13$^{th}$ century: it has been demonstrated by previous works that from the 12$^{th}$ to the 13$^{th}$ century a change in the cobalt supply occurred and thus from the 13$^{th}$ century, cobalt was extracted from the Freiberg mines in Germany, characterized by the presence of specific trace elements: Zn, Pb and In.(Bidegaray and Pollard, 2018; Gratuze et al., 2018, 1995; Neri et al., 2019) No significant amounts of nickel are found (less than 50ppm, see SI) in agreement with the absence of $Ni^{2+}$ absorption bands in the optical spectrum.(Galoisy et al., 2005)

The mined cobalt was traded and probably added to the glass pot as *saffre*: a burnt cobalt ore mixed with sand. (Delamare, 2008; Gratuze et al., 2018) The composition of the *saffre* calculated from the analysis of ceramics decorations for the 13$^{th}$-14$^{th}$ centuries period (Gratuze et al., 1996) suggests the following ratios between the mass compositions: m(CoO) / m(ZnO) = m(CoO) / m(PbO) = 0.66, m(CoO) / m($Fe_2O_3$) = 0.2; m(CoO) / m($In_2O_3$)= 10.2. The results of the linear regression fitting of the composition data from the blue glasses and colorless glasses are given in Figure 9 and agree with the calculated concentration ratios according to the estimated composition of *saffre*. These strong correlations across all samples of blue glass suggest the use of the same cobalt source for all of them. We note however that although the slope of the linear correlation between the iron and cobalt contents agrees with the *saffre* composition, the correlation factor is rather low. This might be explained by the fact that iron is also an important impurity from other raw materials and as a result strong variations arise from the raw materials. The relation between cobalt and lead contents does not show a clear correlation either, compared with the expected *saffre* composition (the expected relation is plotted in Figure 9b with a dashed line). In particular, we observe that for light blue glasses, the lead to cobalt ratio is larger than the ratio found in *saffre*.

Copper is another blue colorant of blue glass. In the present case, we demonstrate that copper is not playing any role as blue colorant in these glasses and is an impurity associated to Zn. The chemical composition of the blue glasses indicates that the Cu content varies between 0.1-0.2wt.%. Copper can be present in the glass in 3 different oxidation states: $Cu^0$, forming metallic nano-particles (Kunicki-Goldfinger et al., 2014) (see the red glass section), $Cu^+$ which is colorless (Hunault et al., 2016a, 2017a) and $Cu^{2+}$ which gives a blueish or greenish hue.(Hunault and Loisel, 2020) The possible contribution of $Cu^{2+}$ absorption, which is expected around 13000$cm^{-1}$ (see green glass section), is difficult to assess since it overlaps with $Fe^{2+}$ (Figure 8c). According to previous studies,(Hunault et al., 2016a) the redox conditions of blue medieval glasses favor $Cu^+$ oxidation state and a negligible contribution of $Cu^{2+}$. Therefore, the presence of copper in the blue glasses is likely not directly related to the color. We observe some correlation between Cu and Zn in blue glasses (Figure 9c) suggesting that both elements might be bound to the same origin. Although the association of zinc with cobalt has been well described,(Gratuze et al., 2018, 1995) the origin of these impurities has been less discussed. So far, copper was not identified as a significant impurity from the cobalt source along with zinc. Here, the association of copper and zinc suggests a common source, for instance as brass. Hence, we could hypothesize that copper and zinc co-occur with cobalt either as impurities from the original ore or as impurities coming from brass tools used in the *saffre* elaboration process.

Most blue glasses belong either to clusters #4 or #5. They are characterized by a relatively high sodium content compared to the other glasses (Figure 4b). However, the absence of any significant correlation between the Na and Co contents prevents us from concluding on a relation between the additions of these elements. This supports that, as mentioned above, the sodium-enriched glasses are not specifically blue glasses and the presence of glasses of similar sodium content but of different colors in the Sainte-Chapelle in Paris. Regarding the cobalt source, we cannot distinguish between the two clusters. Furthermore the two ancient blue glasses with the lowest sodium content (clusters #2 and #3) follow the same *saffre* impurity content. This suggests that, if different, the glasshouses that produced these blue glasses used the same cobalt supply from Germany. This would thus suggest that either these glasshouses were geographically close or that the German provider had a monopole of supply over a large region of France.

### 3.4.3. Green glasses

Green glass was mainly used for clothes and in fewer cases for the walls of buildings, trees, or shoes. All ancient green glasses show similar optical absorption spectra (Figure 10) with a characteristic absorption band from divalent copper ions centered at 13000$cm^{-1}$ (770nm), corresponding to the absorption of red wavelengths. This assignment agrees with the high concentration of copper found in the green glasses (between 1.5-2 wt.% of total CuO) (Figure 10). Although $Cu^{2+}$ alone gives a blue color to glass,(Bamford, 1977; Hunault and Loisel, 2020; Smirniou and Rehren, 2013) the combination with the absorption of the blue wavelengths revealed by the optical spectrum results creates a light transmission window in the green around 18000$cm^{-1}$ (550nm). The high energy absorption is assigned to $Fe^{3+}$.(Hunault and Loisel, 2020) Compared to blue glasses, the absorption from $Fe^{3+}$ is more intense. This is assigned to the higher $Fe^{3+}$ concentration in green glass in agreement with the redox interaction between iron and copper. Indeed, high copper concentration is necessary to oxidize completely all iron in the green glass such as it remains an excess of $Cu^{2+}$ to color the glass.

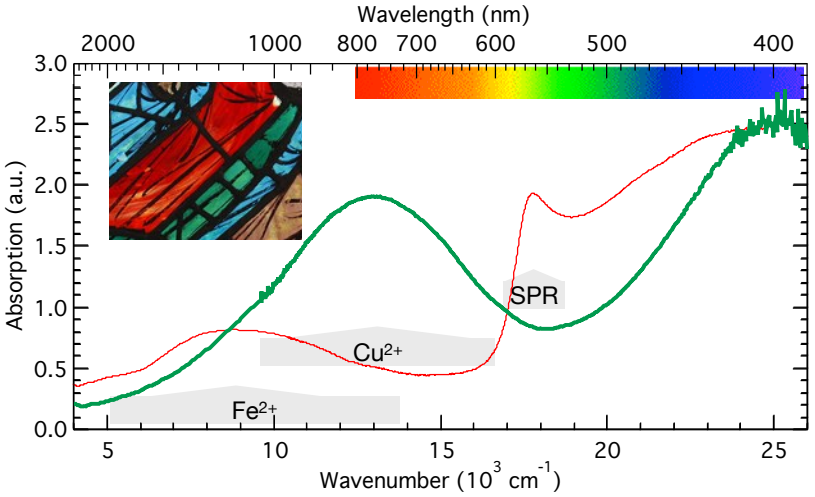



**Figure 10:** *Optical absorption spectra of green and red glasses with the corresponding assignment of the features. Inset: Detail of a panel showing the red and green glasses;*

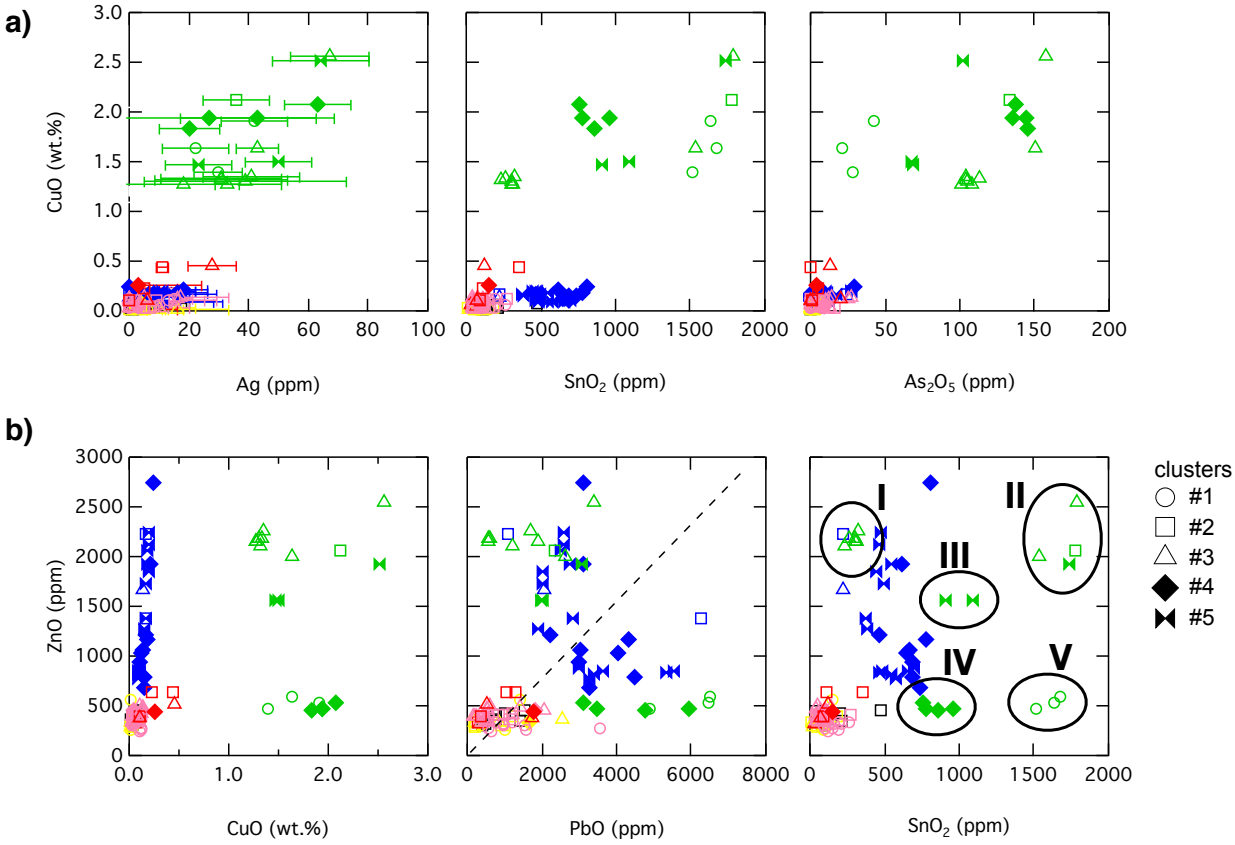



**Figure 11:** *Chemical composition of the glasses obtained by PIXE at the New AGLAE facility a) Copper vs. silver, tin and arsenic contents; b) Zinc vs copper, lead and tin contents. Unless indicated, the error bars are of the size of the markers.*

The use of copper to color glass in green is confirmed by the ancient treatises of Eraclius and Neri.(Vassas, 1971) Both texts report the use of calcined brass (copper-zinc alloy). It is of interest to compare the concentration of trace elements (Figure 11) in light of the clusters identified according to the glass matrix. Silver, tin and zinc, present as $Ag^{+}$, $Zn^{2+}$ and $Sn^{4+}$ respectively, do not contribute to the color of the glass. Thus those elements are not added on purpose for the color but are likely brought by the copper source. In the $Sn_2O$-ZnO graph, we can distinguish five groups of green glasses. These groups fairly agree with the clusters defined by HCA according to the glass matrix. We find that the co-occurrence of copper and

silver, zinc and arsenic at higher concentrations than in colorless glasses for green glasses from clusters #2, #3 and #5. However, green glasses from clusters #1 and #4 show low zinc content similar to colorless glasses, ruling out the use of brass in favor of another copper alloy. Green glasses from cluster #1 contain high tin content suggesting the use of a bronze alloy. The presence of up to 60ppm of Ag in the green glasses suggests that the copper arises from silver mines.(Bourgarit and Thomas, 2012; Craddock, 1985) Lead, another element part of the copper metallurgy, is also found in significant amounts in green glasses (Figure 11b). It is anti-correlated with the zinc content, forming two distinct groups: low zinc-high lead and high lead-low zinc. It is the zinc-tin oxide binary plot that most clearly presents distinct groups of glasses: we can define five groups of green glasses that have specific glass matrix compositions and trace element contents (labeled from I to V in Figure 11b). Altogether we find that the green glasses are marked by significantly different trace element contents. However, these groups do not correlate with a particular panel or window but correspond to glasses from different panels and different windows. This suggests that the four windows were glazed simultaneously using the same glass stock supporting the existence of a large glazing atelier where an important number of workers were collaborating.

### 3.4.4. Red glasses

In the studied windows, red glass was used for the branches and leaves of trees, clothes and boots and for ornamental edges of the panels. All red glasses show a heterogeneous flame-like pattern (Figure 10) that is called striated or “feuilleté”.(Kunicki-Goldfinger et al., 2014) This technique was used from the 12$^{th}$ to the 14$^{th}$ century. Another technique for making red glass is called “plaqué”: a flashed glass consisting in a thin layer of red on a thick layer of supporting colorless glass. The latter was not found among the stained glass of the Sainte-Chapelle in Paris. Both glass manufacturing techniques have one common goal: allowing red glass to be translucent. Indeed, the red glasses show the characteristic absorption band of the surface plasmon resonance (SPR) at 17800cm$^{-1}$ (562nm) (Figure 10). The SPR is assigned to metallic copper nanoparticles. The average size of the nanoparticles can be derived from the shape of the plasmon resonance, using the equation $R = V_f\lambda_p^2/(2\pi c\Delta\lambda)$, where R is the average radius of the metallic nanoparticles, $V_f$ is the Fermi velocity of the electrons in bulk metal (for Cu, $V_f = 15.7 \times 10^5$ cm s$^{-1}$)(Kaye and Laby, 1948), $\lambda_p$ is the peak position wavelength of the resonance, $\Delta\lambda$ is the full width at half-maximum of the absorption band (here 20 nm), and c is the speed of light. This equation predicts that the average size of Cu nanoparticles should be around 15 nm, in agreement with the transmission electron microscope (TEM) observations from Kunicki et al.(Kunicki-Goldfinger et al., 2014)

The absorption from the SPR is intense and therefore the making of translucent red glasses requires a low concentration of nanoparticles or the elaboration of thin layers. Because of this strong light absorption, the luminance L* is lower than 50 for most red glasses (Figure 2). The optical absorption spectrum also shows the absorption band of $Fe^{2+}$ centered near 9000cm$^{-1}$ (1100nm).

Compared to the green glasses, in most red glasses the measured concentration is as low as in colorless glasses (Figure 11), except two glasses reaching a maximum of 4500ppm. This value is lower than the concentration in other studies.(Hunault et al., 2017a; Kunicki-Goldfinger et al., 2014) The impossibility to detect significantly high Cu concentrations likely results from the complex layered microstructure of the type-A “feuilleté” glasses (Kunicki-Goldfinger et al., 2014) compared to the PIXE probing depth: the concentration determined by PIXE is an average over both the colorless and the red layers. The chemical composition of the red layer that could be probed does not reveal any specific presence of reducing species in agreement with the fabrication process of Type-A red glasses. Eventually, we note that the red glasses from the Sainte-Chapelle in Paris have a low CaO content similarly to most of the “Type-A” glasses reported by Kunicki et al.(Kunicki-Goldfinger et al., 2014). All these glasses belong to the same medieval period, the 12 and 13$^{th}$ centuries.

# 4. Conclusions

The restoration of the windows of the nave of the Sainte-Chapelle in Paris was a unique opportunity to perform an in depth investigation of the chemistry and color of these glasses. With 105 glasses analyzed, we report the first extensive investigation of the links between chemistry and color of Thirteenth Century glasses from the Saint-Chapelle in Paris. These data were obtained using a combination of non-destructive techniques: PIXE-PIGE provides access to a wide range of chemical elements, and optical absorption spectroscopy determines the nature of the coloring species. Our results significantly complete the few other dataset already published.(Lagabrielle and Velde, 2005; Verita et al., 2005)

The conclusions can be further summarized as follows:

- All ancient glasses have a potash-type chemical composition arising from a wood-ash glass recipe in agreement with ancient medieval glassmaking treatises. The concentrations of major and minor elements suggest the use of beech and bracken ashes.
- Hierarchical cluster analysis (HCA) allowed to define clusters of glasses of distinct glass matrix chemical compositions. The low composition variability within each cluster, suggests that it corresponds to a distinct bundle of glass. The chromophores and related impurities for a given color form various sub-groups, which often correlate with the clusters, supporting that glasses within a cluster originate from the same glasshouse. Whether or not these different bundles originate from the same glasshouse is still difficult to confirm yet cannot be ruled out.
- A distinct compositional sub-group of glasses shows enriched sodium content. All but a few of these glasses are blue glasses. The origin of the sodium remains unclear but might indicate a distinct glasshouse origin, in Normandy, France. However, the fact that this characteristic composition pattern is found in other windows in other colors supports that this is not specific to the production of blue glasses and that the entire glazing project, although achieved by different ateliers (glaziers), was supported by a unique glass supply.
- Colorless, purple and yellow colors arise from a subtle mastering of the manganese and iron redox ratios.
- Blue glasses form two distinct color-hue groups: dark blue glasses are colored by cobalt and light blue glasses are colored by lower cobalt contents and reduced iron. In all cases, Co, Zn and In contents are correlated suggesting the use of *saffre* from the German mines of Freiberg. The blue glasses are mainly split into two chemical composition clusters but the Co source impurities follow a unique correlation suggesting that both sub-groups of blue glasses could originate from the same glasshouse. It could alternatively imply that different glasshouses used the same cobalt source and would confirm the monopole of Germany as a cobalt supplier during the $13^{th}$ century.
- Green glasses are colored by divalent copper. The impurities arising from the copper source enable to distinguish bundles of glass that fairly agree with the HCA clusters. This further supports that the clusters correspond to bundles of glass that were used to glaze the different windows simultaneously.
- Red glasses are “striated” glasses colored by metallic copper nanoparticles as observed in the $12^{th}$-$13^{th}$ centuries.
- Former painting style analyses published by art historians, suggest that the same atelier glazed the four northern windows.(Grodecki and Brisac, 1984) The clusters and sub-groups of glasses are not specific to a panel or a window, which confirms that the glazing work of at least these four windows was conducted in parallel.

Altogether, the obtained chemical data overcome the lack of historiography and provide substantial additional evidences of the organization of the glazing process conducted in a record time of a few years: the glazing work of all the windows of the nave, although achieved probably by the cooperation of several ateliers, used a common glass supply.

Other analytical techniques like electron micro-probe analysis (EMPA) or LA-ICP-MS could provide additional compositional information on trace elements such as rare-earth, already used for determining the origin of ancient glasses.(Wedepohl et al., 2011a, 2011b) However, this method requires the sampling of the glasses. Even if this could be considered to some extent, then only a restrained number of glasses would be selected to allow sampling the edge of the glass piece for instance. Hence sampling a glass piece from the center of the panel would require dismantling the panel or process to a very delicate endeavor of extracting one specific glass piece. Anyway, such procedure would not allow the access to a large number of glasses as it has been done in the present study thanks to the non-invasive IBA techniques at the New AGLAE facility.

Further investigations are required to provide a complete archaeological significance to the chemical composition data. Comparison of these results with those of other contemporary buildings should allow to complete our understanding of the history of medieval art and stained glasses across France: trades of materials, sharing of knowledge and evolution of techniques, which are already acknowledged in the studies of the art historians for the inventory of stained glass. In particular, further studies on the chemical composition variations within glasshouses as found in excavations in combination with investigations of the influence of the raw materials would complete with quantitative definitions what Jackson et al.(Jackson et al., 2005) had defined earlier as the “natural” and “behavioral” variability.

# Acknowledgements

This work was supported by the Convergence project “VITRAUX” (SU-14-R-ScPC-15-2) from Sorbonne Universités. The IBA analyses were performed at the New AGLAE facility (ANR-10-EQPX-22). The authors thank Isabelle Pallot-Frossard for her continuous support and interest in this project. M.O.J.Y.H. thanks François Guilhem and Serge Cohen for precious advises in the data analysis using R software. Finally, the authors gratefully thank the two anonymous reviewers who helped improve and clarify this paper to a great extent.


# Supporting information

Restoration charts; dendrograms obtained using R and analysis of the clusters; comparison with previous data. Chemical composition raw data; R code used for interpretation.

# References


Adlington, L.W., Freestone, I.C., 2017. Using handheld pXRF to study medieval stained glass: A methodology using trace elements. MRS Adv. 2, 1785–1800. https://doi.org/10.1557/adv.2017.233

Adlington, L.W., Freestone, I.C., Kunicki-Goldfinger, J.J., Ayers, T., Gilderdale Scott, H., Eavis, A., 2019. Regional patterns in medieval European glass composition as a provenancing tool. J. Archaeol. Sci. 110, 104991. https://doi.org/10.1016/j.jas.2019.104991

Aubert, M., Grodecki, L., Lafond, J., Verrier, J., 1959. Les Vitraux de Notre-Dame et de la Sainte-Chapelle de Paris, Corpus vitrearum Medii Aevi. Caisse nationale des monuments historiques Centre national de la recherche scientifique, Paris.

Bamford, C.R., 1977. Colour Generation and Control in Glass. Elsevier Scientific Publishing Company : distributors for the U.S. and Canada, Elsevier North-Holland.

Bidegaray, A.-I., Godet, S., Bogaerts, M., Cosyns, P., Nys, K., Terryn, H., Ceglia, A., 2019. To be purple or not to be purple? How different production parameters influence colour and redox in manganese containing glass. J. Archaeol. Sci. Rep. 27, 101975. https://doi.org/10.1016/j.jasrep.2019.101975

Bidegaray, A.-I., Nys, K., Silvestri, A., Cosyns, P., Meulebroeck, W., Terryn, H., Godet, S., Ceglia, A., 2020. 50 shades of colour: how thickness, iron redox and manganese/antimony contents influence perceived and intrinsic colour in Roman glass. Archaeol. Anthropol. Sci. 12, 109. https://doi.org/10.1007/s12520-020-01050-0

Bidegaray, A.-I., Pollard, A.M., 2018. Tesserae Recycling in the Production of Medieval Blue Window Glass. Archaeometry 60, 784–796. https://doi.org/10.1111/arcm.12350

Bingham, P.A., Jackson, C.M., 2008. Roman blue-green bottle glass: chemical–optical analysis and high temperature viscosity modelling. J. Archaeol. Sci. 35, 302–309. https://doi.org/10.1016/j.jas.2007.03.011

Bontemps, G., 1868. Guide du verrier : traité historique et pratique de la fabrication des verres, cristaux, vitraux / par G. Bontemps,... Librairie du “Dictionnaire des arts et manufactures” (Paris).

Bourgarit, D., Thomas, N., 2012. Late medieval copper alloying practices: a view from a Parisian workshop of the 14th century AD. J. Archaeol. Sci. 39, 3052–3070. https://doi.org/10.1016/j.jas.2012.04.009

Calligaro, T., 2008. PIXE in the study of archaeological and historical glass. X-Ray Spectrom. 37, 169–177. https://doi.org/10.1002/xrs.1063

Capobianco, N., Hunault, M.O.J.Y., Balcon-Berry, S., Galoisy, L., Sandron, D., Calas, G., 2019. The Grande Rose of the Reims Cathedral: an eight-century perspective on the colour management of medieval stained glass. Sci. Rep. 9, 3287. https://doi.org/10.1038/s41598-019-39740-y

Cox, G.A., Gillies, K.J.S., 1986. The X-Ray Fluorescence Analysis of Medieval Durable Blue Soda Glass from York Minster. Archaeometry 28, 57–68. https://doi.org/10.1111/j.1475-4754.1986.tb00374.x

Craddock, P.T., 1985. Medieval Copper Alloy Production and West African Bronze Analyses - Part I. Archaeometry 27, 17–41. https://doi.org/10.1111/j.1475-4754.1985.tb00344.x

Delamare, F., 2008. Bleus en poudres: de l’art à l’industrie : 5000 ans d’innovations. Presses des MINES.

Fleming, S.J., Swann, C.P., 1987. Color additives and trace elements in ancient glasses: Specialized studies using PIXE spectrometry. Nuclear Instruments and Methods in Physics Research Section B: Beam Interactions with Materials and Atoms 22, 411–418. https://doi.org/10.1016/0168-583X(87)90368-5

Freestone, I., Price, J., Cartwright, C., 2009. The batch: its recognition and significance, in: Janssens, K.H.A., Congrès international d’étude historique du verre, International Association for the History of Glass (Eds.), Annales Du 17e Congrès de l’Association Internationale Pour l’Histoire Du Verre, Anvers, 2006 =: Annales of the 17th Congress of

884 the International Association for the History of Glass, 2006, Antwerp. University Press
885 Antwerp, Antwerp, pp. 130–135.
886 Freestone, I.C., 1992. Theophilus and the Composition of Medieval Glass, in: Symposium J –
887 Materials Issues in Art and Archaeology III, MRS Online Proceedings Library.
888 https://doi.org/10.1557/PROC-267-739
889 Galoisy, L., Calas, G., Cormier, L., Marcq, B., Thibault, M.H., 2005. Overview of the environment
890 of Ni in oxide glasses in relation to the glass colouration. Physics and Chemistry of Glasses
891 46, 394–399.
892 Gliozzo, E., 2016. The composition of colourless glass: a review. Archaeol. Anthropol. Sci. 1–29.
893 https://doi.org/10.1007/s12520-016-0388-y
894 Gratuze, B., 2013. Provenance Analysis of Glass Artefacts, in: Janssens, K. (Ed.), Modern Methods
895 for Analysing Archaeological and Historical Glass. John Wiley & Sons Ltd, pp. 311–343.
896 Gratuze, B., Pactat, I., Schibille, N., 2018. Changes in the Signature of Cobalt Colorants in Late
897 Antique and Early Islamic Glass Production. Minerals 8, 225.
898 https://doi.org/10.3390/min8060225
899 Gratuze, B., Soulier, I., Barrandon, J.N., Foy, D., 1995. The origin of cobalt blue pigments in french
900 glass from the thirteenth to the eighteenth centuries. Trade and discovery: the scientific
901 study of artefacts from post-medieval Europe and beyond 123–33.
902 Gratuze, B., Soulier, I., Blet, M., Vallauri, L., 1996. De l'origine du cobalt: du verre à la céramique.
903 Revue d'archéométrie 77–94.
904 Grodecki, L., 1976. Le chapitre XXVIII de la Schedula du moine Théophile: technique et esthétique
905 du vitrail roman. Comptes rendus des séances de l'Académie des Inscriptions et Belles-
906 Lettres 120, 345–357. https://doi.org/10.3406/crai.1976.13258
907 Grodecki, L., Brisac, C., 1984. Le vitrail gothique: au XIIIème siècle. Vilo/office du livre.
908 Hawthorne, J.G., Smith, C.S., 1979. Theophilus on Divers Arts: the foremost medieval treatise on
909 painting, glassmaking and metal-work. Translated from the Latin with introduction and
910 notes, Dover Publications, Inc. ed. New York.
911 Hunault, M., Bauchau, F., Loisel, C., Hérold, M., Galoisy, L., Newville, M., Calas, G., 2016a.
912 Spectroscopic Investigation of the Coloration and Fabrication Conditions of Medieval Blue
913 Glasses. J. Am. Ceram. Soc. 99, 89–97. https://doi.org/10.1111/jace.13783
914 Hunault, M., Calas, G., Galoisy, L., Lelong, G., Newville, M., 2014. Local Ordering Around
915 Tetrahedral Co2+ in Silicate Glasses. J. Am. Ceram. Soc. 97, 60–62.
916 https://doi.org/10.1111/jace.12709
917 Hunault, M., Lelong, G., Gauthier, M., Gélébart, F., Ismael, S., Galoisy, L., Bauchau, F., Loisel, C.,
918 Calas, G., 2016b. Assessment of Transition Element Speciation in Glasses Using a Portable
919 Transmission Ultraviolet–Visible–Near-Infrared (UV-Vis-NIR) Spectrometer. Appl
920 Spectrosc 70, 778–784. https://doi.org/10.1177/0003702816638236
921 Hunault, M.O.J.Y., Loisel, C., 2020. Looking through model medieval green glasses: From color to
922 recipe. International Journal of Applied Glass Science 11, 463–470.
923 https://doi.org/10.1111/ijag.15134
924 Hunault, M.O.J.Y., Loisel, C., Bauchau, F., Lemasson, Q., Pacheco, C., Pichon, L., Moignard, B.,
925 Boulanger, K., Hérold, M., Calas, G., Pallot-Frossard, I., 2017a. Nondestructive Redox
926 Quantification Reveals Glassmaking of Rare French Gothic Stained Glasses. Anal. Chem.
927 https://doi.org/10.1021/acs.analchem.7b01452
928 Hunault, M.O.J.Y., Vinel, V., Cormier, L., Calas, G., 2017b. Thermodynamic insight into the
929 evolution of medieval glassworking properties. J. Am. Ceram. Soc. 89, 6277–6284.
930 https://doi.org/10.1111/jace.14819
931 Jackson, C.M., 2005. Making Colourless Glass in the Roman Period*. Archaeometry 47, 763–780.
932 https://doi.org/10.1111/j.1475-4754.2005.00231.x
933 Jackson, C.M., Booth, C.A., Smedley, J.W., 2005. Glass by design? Raw materials, recipes and
934 compositional data. Archaeometry 47, 781–795.

Jackson, C.M., Smedley, J.W., 2008. Medieval and post-medieval glass technology: seasonal changes in the composition of bracken ashes from different habitats through a growing season. Glass Technology-European Journal of Glass Science and Technology Part A 49, 240–245.
Jackson, C.M., Smedley, J.W., 2004. Medieval and post-medieval glass technology: melting characteristics of some glasses melted from vegetable ash and sand mixtures. Glass Technol.: Eur. J. Glass Sci. Technol., Part A 45, 36–42.
Jembrih-Simbürger, D., Neelmeijer, C., Schalm, O., Fredrickx, P., Schreiner, M., De Vis, K., Mäder, M., Schryvers, D., Caen, J., 2002. The colour of silver stained glass—analytical investigations carried out with XRF, SEM/EDX, TEM, and IBA. J. Anal. At. Spectrom. 17, 321–328. https://doi.org/10.1039/B111024C
Kaye, G.W.C., Laby, T.H., 1948. Tables of physical and chemical constants and some mathematical functions. London, Royaume-Uni de Grande-Bretagne et d'Irlande du Nord.
Kuisma-Kursula, P., 2000. Accuracy, precision and detection limits of SEM–WDS, SEM–EDS and PIXE in the multi-elemental analysis of medieval glass. X-Ray Spectrometry 29, 111–118. https://doi.org/10.1002/(SICI)1097-4539(200001/02)29:1<111::AID-XRS408>3.0.CO;2-W
Kunicki-Goldfinger, J., Kierzek, J., Kasprzak, A., Małżewska-Bućko, B., 2000. A study of eighteenth century glass vessels from central Europe by x-ray fluorescence analysis. X-Ray Spectrometry 29, 310–316. https://doi.org/10.1002/1097-4539(200007/08)29:4<310::AID-XRS431>3.0.CO;2-E
Kunicki-Goldfinger, J.J., Freestone, I.C., McDonald, I., Hobot, J.A., Gilderdale-Scott, H., Ayers, T., 2014. Technology, production and chronology of red window glass in the medieval period – rediscovery of a lost technology. J. Archaeol. Sci. 41, 89–105. https://doi.org/10.1016/j.jas.2013.07.029
Lagabrielle, S., Velde, B., 2005. Evolution of French stained glass compositions during the middle Ages - Analyses and observations made on the Cluny collection, in: Annales Du 16e Congrès de l'Association Internationale Pour l'Histoire Du Verre. pp. 341–346.
Lautier, C., Kurmann-Schwarz, B., 2010. Recherches récentes sur le vitrail médiéval, 1998-2009. 2e partie. Kunstchronik 63, 313–338.
Lautier, C., Sandron, D., 2008. Antoine de Pise: l'art du vitrail vers 1400. CTHS, Comité des travaux historiques et scientifiques.
Loisel, C., 2020. La Sainte-Chapelle de Paris : Analyser et restaurer pour conserver ce joyau. Beaux-Arts Editions 32–35.
Molina, G., Murcia, S., Molera, J., Roldan, C., Crespo, D., Pradell, T., 2013. Color and dichroism of silver-stained glasses. J Nanopart Res 15, 1932. https://doi.org/10.1007/s11051-013-1932-7
Musso, P., 2017. La Religion industrielle: Monastère, manufacture, usine. Une généalogie de l'entreprise, Fayard. ed. Paris, France.
Nelson, C., White, W., 1980. Transition metal ions in silicate melts—I. Manganese in sodium silicate melts□. Geochim. Cosmochim. Acta 44, 887–893. https://doi.org/10.1016/0016-7037(80)90269-0
Neri, E., Gratuze, B., Schibille, N., 2019. The trade of glass beads in early medieval Illyricum: towards an Islamic monopoly. Archaeol. Anthropol. Sci. 11, 1107–1122. https://doi.org/10.1007/s12520-017-0583-5
Pallot-Frossard, I., 1998. La place du vitrail dans l'architecture ?, in: Le Matériau Vitreux : Verre et Vitraux / Actes Du Cours Intensif Européen, Ravello, 28-30 Avril 1995. Bari : Edipuglia, Centro universitario europeo per i beni culturali, Ravello, pp. 23–42.
Panofsky, E., 1946. Abbot Suger on the Abbey Church of St.-Denis and its art treasures. Princeton University Press, Princeton (N.J.), Etats-Unis.
Paynter, S., Jackson, C.M., 2018. Mellow yellow: An experiment in amber. J. Archaeol. Sci. Rep. 22, 568–576. https://doi.org/10.1016/j.jasrep.2017.11.038

Pérez-Villar, S., Rubio, J., Oteo, J.L., 2008. Study of color and structural changes in silver painted medieval glasses. J. Non-Cryst. Solids 354, 1833–1844. https://doi.org/10.1016/j.jnoncrysol.2007.10.008
Phelps, M., Freestone, I.C., Gorin-Rosen, Y., Gratuze, B., 2016. Natron glass production and supply in the late antique and early medieval Near East: The effect of the Byzantine-Islamic transition. J. Archaeol. Sci. 75, 57–71. https://doi.org/10.1016/j.jas.2016.08.006
Pichon, L., Calligaro, T., Lemasson, Q., Moignard, B., Pacheco, C., 2015. Programs for visualization, handling and quantification of PIXE maps at the AGLAE facility. Nucl. Instrum. Methods Phys. Res., Sect. B. https://doi.org/10.1016/j.nimb.2015.08.086
Pichon, L., Moignard, B., Lemasson, Q., Pacheco, C., Walter, P., 2014. Development of a multi-detector and a systematic imaging system on the AGLAE external beam. Nucl. Instrum. Methods Phys. Res., Sect. B 318, 27–31. https://doi.org/10.1016/j.nimb.2013.06.065
Rehren, T., Brüggler, M., 2015. Composition and production of late antique glass bowls type Helle. J. Archaeol. Sci. Rep. 3, 171–180. https://doi.org/10.1016/j.jasrep.2015.05.021
Rehren, Th., Freestone, I.C., 2015. Ancient glass: from kaleidoscope to crystal ball. J. Archaeol. Sci., Scoping the Future of Archaeological Science: Papers in Honour of Richard Klein 56, 233–241. https://doi.org/10.1016/j.jas.2015.02.021
Royce-Roll, D., 1994. THE COLORS OF ROMANESQUE STAINED GLASS. Journal of Glass Studies 3, 71–80.
Schalm, O., Caluwé, D., Wouters, H., Janssens, K., Verhaeghe, F., Pieters, M., 2004. Chemical composition and deterioration of glass excavated in the 15th–16th century fishermen town of Raversijde (Belgium). Spectrochim. Acta, Part B 59, 1647–1656. https://doi.org/10.1016/j.sab.2004.07.012
Schalm, O., Janssens, K., Wouters, H., Caluwé, D., 2007. Composition of 12–18th century window glass in Belgium: Non-figurative windows in secular buildings and stained-glass windows in religious buildings. Spectrochim. Acta, Part B 62, 663–668. https://doi.org/10.1016/j.sab.2007.03.006
Schibille, N., Meek, A., Tobias, B., Entwistle, C., Avisseau-Broustet, M., Da Mota, H., Gratuze, B., 2016. Comprehensive Chemical Characterisation of Byzantine Glass Weights. PLoS ONE 11, e0168289. https://doi.org/10.1371/journal.pone.0168289
Schreiber, H.D., 1986. Redox processes in glass-forming melts. J. Non-Cryst. Solids 84, 129–141.
Schreurs, J.W.H., Brill, R.H., 1984. Iron and Sulfur Related Colors in Ancient Glasses. Archaeometry 26, 199–209. https://doi.org/10.1111/j.1475-4754.1984.tb00334.x
Sellner, C., Oel, H., Camara, B., 1979. Untersuchung alter Gläser (Waldglas) auf Zusammenhang von Zusammensetzung, Farbe und Schmelzatmosphäre mit der Elektronenspektroskopie und der Elektronenspinresonanz (ESR). Glastechn. Ber. 52, 255–264.
Smedley, J.W., Jackson, C.M., 2002. Medieval and post-medieval glass technology: a review of bracken in glassmaking. Glass Technology 43, 221–224.
Smedley, J.W., Jackson, C.M., Booth, C.A., 1998. BACK TO THE ROOTS : THE RAW MATERIALS, GLASS RECIPES AND GLASSMAKING PRACTICES OF THEOPHILUS, in: Prehistory and History of Glassmaking Technology, Ceramics and Civilization. Presented at the 99th Annual meeting of the American Ceramic Society, American Ceramic Society, pp. 145–166.
Smirniou, M., Rehren, T., 2013. Shades of blue – cobalt-copper coloured blue glass from New Kingdom Egypt and the Mycenaean World: a matter of production or colorant source? J. Archaeol. Sci. 40, 4731–4743. https://doi.org/10.1016/j.jas.2013.06.029
Smith, E.B., 2015. ‘All my stained glass which I brought from Europe’: William Poyntell and the Sainte-Chapelle medallions. HISCOL 27, 323–334. https://doi.org/10.1093/jhc/fhu049
Stern, W.B., Gerber, Y., 2004. Potassium–Calcium Glass: New Data and Experiments*. Archaeometry 46, 137–156. https://doi.org/10.1111/j.1475-4754.2004.00149.x
Theophilus, 1847. Diversarum artium schedula. J. Murray.

Tite, M.S., Shortland, A., Maniatis, Y., Kavoussanaki, D., Harris, S.A., 2006. The composition of the soda-rich and mixed alkali plant ashes used in the production of glass. J. Archaeol. Sci. 33, 1284–1292. https://doi.org/10.1016/j.jas.2006.01.004

Van Wersch, L., Loisel, C., Mathis, F., Strivay, D., Bully, S., 2016. Analyses of Early Medieval Stained Window Glass From the Monastery of Baume-Les-Messieurs (Jura, France). Archaeometry 58, 930–946. https://doi.org/10.1111/arcm.12207

Vassas, C.D., 1971. Etude chimique, thermographique et physique de verres de vitraux du Moyen-Age, in: Communications scientifiques et techniques. Presented at the Congrés international du verre, Versailles, France.

Vercamer, V., Lelong, G., Hijiya, H., Kondo, Y., Galoisy, L., Calas, G., 2015. Diluted Fe3+ in silicate glasses: Structural effects of Fe-redox state and matrix composition. An optical absorption and X-band/Q-band EPR study. J. Non-Cryst. Solids 428, 138–145. https://doi.org/10.1016/j.jnoncrysol.2015.08.010

Verita, M., Nicola, C., Sommariva, G., 2005. The stained glass windows of the Sainte Chapelle in Paris: Investigations on the origin of the loss of the painted work, in: Annales Du 16e Congrès de l'Association Internationale Pour l'Histoire Du Verre. pp. 347–351.

Vilarigues, M., Coutinho, I., Medici, T., Alves, L.C., Gratuze, B., Machado, A., 2019. From beams to glass: determining compositions to study provenance and production techniques. Physical Sciences Reviews 0. https://doi.org/10.1515/psr-2018-0019

Vilarigues, M., da Silva, R.C., 2004. Ion beam and infrared analysis of medieval stained glass. Appl. Phys. A 79, 373–378. https://doi.org/10.1007/s00339-004-2538-9

Wedepohl, K.H., Simon, K., 2010. The chemical composition of medieval wood ash glass from Central Europe. Chemie der Erde - Geochemistry 70, 89–97. https://doi.org/10.1016/j.chemer.2009.12.006

Wedepohl, K.H., Simon, K., Kronz, A., 2011a. Data on 61 Chemical Elements for the Characterization of Three Major Glass Compositions in Late Antiquity and the Middle Ages. Archaeometry 53, 81–102. https://doi.org/10.1111/j.1475-4754.2010.00536.x

Wedepohl, K.H., Simon, K., Kronz, A., 2011b. The chemical composition including the Rare Earth Elements of the three major glass types of Europe and the Orient used in late antiquity and the Middle Ages. Geochemistry 71, 289–296. https://doi.org/10.1016/j.chemer.2011.04.001